

1 **A new method for amino acid geochronology of the shell of the bivalve** 2 **mollusc *Arctica islandica***

3 Martina L. G. Conti¹, Paul G. Butler², David J. Reynolds², Tamara Trofimova², James D. Scourse²,
4 Kirsty E. H. Penkman¹

5 ¹Department of Chemistry, University of York, York, YO10 5DD, United Kingdom

6 ²Centre For Geography and Environmental Science, University of Exeter, United Kingdom

7 Correspondence to: Martina L.G. Conti (martina.conti@york.ac.uk)

8 **Abstract**

9 The bivalve mollusc *Arctica islandica* can live for hundreds of years, and its shell has provided a valuable resource for
10 sclerochronological studies and geochemical analyses for understanding palaeoenvironmental change. Shell specimens
11 recovered from the seabed need to be dated in order to aid sample selection, but existing methods using radiocarbon
12 dating or crossdating are both costly and time-consuming. We have investigated amino acid geochronology (AAG) as
13 a potential alternative means of providing a less costly and more efficient rangefinding method. In order to do this, we
14 have investigated the complex microstructure of the shells, as this may influence the application of AAG. Each of the
15 three microstructural layers of *A. islandica* have been isolated and their protein degradation examined (amino acid
16 concentration, composition, racemisation and peptide bond hydrolysis). The intra-crystalline protein fraction was
17 successfully extracted following oxidation treatment for 48 h, and high temperature experiments at 140°C established
18 coherent breakdown patterns in all three layers, but the inner portion of the outer shell layer (iOSL) was the most
19 appropriate component due to practicalities. Sampling of the iOSL layer in Holocene shells from early and late
20 ontogeny (over 100-400 years) showed that the resolution of AAG is too low in *A. islandica* for within-shell age
21 resolution. However, analysis of 52 subfossil samples confirmed that this approach could be used to establish a relative
22 geochronology for this biomineral throughout the whole of the Quaternary. In the Late Holocene the temporal
23 resolution is ~1500-2000 years. Relative dating of 160 dredged shells of unknown age were narrowed down using
24 AAG as a range finder, showing that a collection of shells from Iceland and the North Sea covered the Middle Holocene,
25 Late Holocene, later and post-medieval (1171-1713 CE) and modern day. This study confirms the value of *A. islandica*
26 as a reliable material for rangefinding and for dating Quaternary deposits.

Short summary

The mollusc *Arctica islandica* can survive for hundreds of years and its annual growth captures environmental conditions, so each shell provides a detailed climatic record. Dating is essential for sample selection, but radiocarbon and crossdating are time-consuming and costly. As an alternative, amino acid geochronology was investigated in the three aragonitic layers forming the shells. This study confirms the value of AAG in the iOSL layer as a method for rangefinder dating Quaternary *A. islandica* shells.

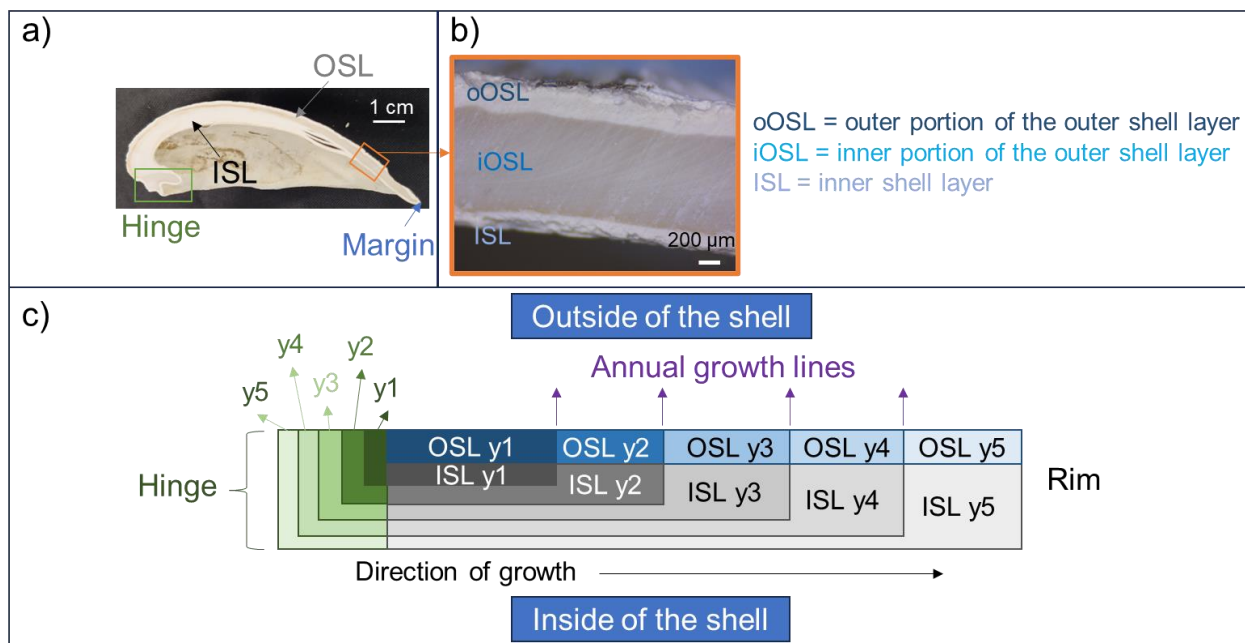
1 Introduction

Arctica islandica (ocean quahog) is a bivalve mollusc that inhabits the continental shelf seas across the North Atlantic region (MarLIN database). It presently lives across subpolar latitudes of the North Atlantic region of Europe from the English Channel to the White Sea, and in North America from Virginia to Nova Scotia (MarLIN database, Schöne, 2013). Its Quaternary subfossil shells are also found in ancient sediments in Northern Europe and in the Mediterranean Sea (Malatesta and Zarlenga, 1986; Eyles et al., 1994; Crippa et al., 2019). *Arctica islandica* has been routinely used for palaeoclimate and palaeoceanographic studies due its exceptionally long life (>500 years maximum longevity; Butler et al, 2013), and its capability to capture climatological changes within its periodic accretions (i.e. growth lines; Witbaard et al., 1997; Schöne et al., 2005a; Schöne, 2013; Butler et al, 2013; Reynolds et al., 2016; Estrella-Martínez et al., 2019). The study of annual and sub-annual band growth variability within the calcium carbonate shells, termed sclerochronology (Fig. 1), provides high-resolution detailed palaeoclimatology data spanning decades to multiple centuries (Schöne et al., 2004; Schöne and Fiebig, 2008; Dunca et al., 2009; Butler et al., 2009, 2013; Wanamaker et al., 2012; Reynolds et al., 2016; Trofimova et al., 2018; Estrella-Martinez et al., 2019; Brosset et al., 2022).

Developing sclerochronological records requires visual and statistical cross-matching across numerous samples; this endeavour can be hugely time consuming and therefore needs to be targeted appropriately, especially when dead-collected samples are of unknown age. Dating of the specimens is essential to develop accurate sclerochronological records: radiocarbon dating can be a very precise technique for Late Quaternary marine shells (back to 40,000-55,000 years). However, this is not always economically viable (Hajdas et al., 2021), especially for a large number of samples, while accurate correction for the marine reservoir effect is required and the dating uncertainty can be a few hundreds of years (Alves et al., 2018). One possible alternative is amino acid geochronology (AAG), a relative-age technique that is comparatively fast and inexpensive. AAG is applicable to mollusc shell deposits spanning the Quaternary period (e.g. Sejrup and Haugen, 1994; Davies et al., 2009; Ortiz et al., 2009; 2015; Penkman, 2010; Demarchi et al., 2013a-b, Bridgland et al., 2013), and can have high precision and resolution in tropical corals (Hendy et al., 2012).

56 AAG dating of biominerals is based on the natural degradation of proteins to determine age; the main processes are
57 racemisation (and epimerisation, both leading to an increase in amino acid D/L), peptide bond hydrolysis, and amino
58 acid decomposition (Hare and Mitterer, 1969). When organisms die, or when there is no more tissue turnover, these
59 degradation reactions occur in tandem. The inter-crystalline fraction of biominerals (Gries et al., 2009), the protein
60 which forms a matrix between the crystallites, is potentially more susceptible to external contamination or leaching,
61 and can compromise the reliability of AAG in some biominerals (Sykes et al., 1995, Penkman et al., 2008; Ortiz et al.,
62 2015). In some materials, a small fraction of the protein is contained within the interstitial voids of the crystal structure
63 and can be isolated with an oxidising pre-treatment; this is defined as the intra-crystalline (IcP) fraction (Towe and
64 Thompson, 1972; Sykes et al., 1995, Penkman et al., 2008; Gries et al., 2009). The IcP can be isolated with oxidation
65 using NaOCl (or H₂O₂ in some cases) and its stability against external contamination and leaching means that, in some
66 biominerals, it effectively operates as a closed-system. The isolation of closed-system IcP has provided reliable
67 chronological information in some gastropods (Penkman et al., 2008; Ortiz et al., 2015; Demarchi et al., 2013a-b;
68 Bridgland et al., 2013), ostracods (Ortiz et al., 2013), corals (Hendy et al., 2012; Tomiak et al., 2013; 2016), eggshell
69 (Brooks et al., 1990; Crisp et al., 2013), enamel (Dickinson et al., 2019; Baleka et al., 2021) and foraminifera (Wheeler
70 et al., 2021), but not in all biominerals (e.g. Orem and Kaufman, 2011; Torres et al., 2013; Demarchi et al., 2015).

71 A further complication for AAG of bivalve shells is that the different microstructural layers in bivalves are likely to be
72 composed of different proteins, and therefore may degrade differently. The *A. islandica* shell comprises a periostracum
73 and three aragonitic layers of differing crystal microstructure (Schöne, 2013): a homogeneous granular structure in the
74 outer portion of the outer shell layer (oOSL), a cross-acicular structure for the inner portion of the outer shell layer
75 (iOSL), and a cross-lamellar to cross-acicular structure for the inner shell layer (ISL; Fig. 1; Dunca et al., 2009; Schöne,
76 2013; Milano et al., 2017b).



77

78 Figure 1. a) cross section of *Arctica islandica* showing the b) inner shell layer (ISL), inner portion of the outer shell
 79 layer (iOSL), and outer portion of the outer shell layer (oOSL); c) simplified schematics of the growth of ISL and OSL
 80 and hinge ("y" indicates the year of growth).

81 *Arctica islandica*, *Glycymeris glycymeris*, *Callista chione* and *Entemnotrochus adansonianus* have shown distinct
 82 racemisation and epimerisation rates which depend on the microstructural layer analysed (Haugen and Sejrup, 1990,
 83 1992; Sejrup and Haugen, 1994; Goodfriend et al., 1995, 1997; Torres et al., 2013; Demarchi et al., 2015). Early
 84 studies without chemical oxidation on *A. islandica* (i.e. combining both the inter-and any intra-crystalline fraction)
 85 showed different epimerisation rates, AA concentrations and composition between the inner and outer layers (Haugen
 86 and Sejrup, 1990, 1992; Sejrup and Haugen, 1994). Intra-shell variability was also high, hypothesised to be due to
 87 microorganism attack of the protein during early stages of diagenesis, external contamination and/or leaching through
 88 micropores (Sejrup and Haugen, 1994; Kosnik and Kaufman, 2008). A study on the use of D/L for ontogenetic studies
 89 of unbleached shells revealed Asp D/L (aspartic acid as referred to by Goodfriend and Weidman, 2001) values higher
 90 in the umbo growth lines (laid down when the shells are young) compared to the rim growth lines (deposited when the
 91 shell is old; Goodfriend and Weidman, 2001). A difference in AA composition between early and late ontogeny was
 92 also observed, indicating the need of sampling standardisation; the recommendation was to sample shells from band
 93 year 20 in the outer shell layer (Goodfriend and Weidman, 2001). Asx D/L values (Asx indicating aspartic acid and
 94 asparagine, that cannot be analytically distinguished due to irreversible deamination) in unbleached *A. islandica* shells

95 collected between 1982 and 1994 were shown to increase with age over a 154-year chronology, highlighting that AAG
96 can potentially help in dating sclerochronologies (Marchitto et al., 2000).

97 Given the variability observed in unbleached *A. islandica* shell AA data, a way forward is to test for the presence of
98 any IcP in *A. islandica* shells, and whether it forms a closed system for individual microstructures (e.g. Torres et al.,
99 2013; Demarchi et al., 2013a-b, 2015; Baldreki et al., 2024). The use of IcP in AAG has not been fully investigated
100 on *A. islandica* (Sykes et al., 1995), and there is variety in sampling strategy for specific microstructural layers (Haugen
101 and Sejrup, 1990, 1992; Sejrup and Haugen, 1994; Marchitto et al., 2000; Goodfriend and Weidman, 2001). If it is
102 possible to isolate an intra-crystalline fraction that exhibits closed-system behaviour from any of the layers in *A.*
103 *islandica* shells, an IcP approach may be able to reduce the intra-shell variability, and increase accuracy.

104 **1.1 Aims**

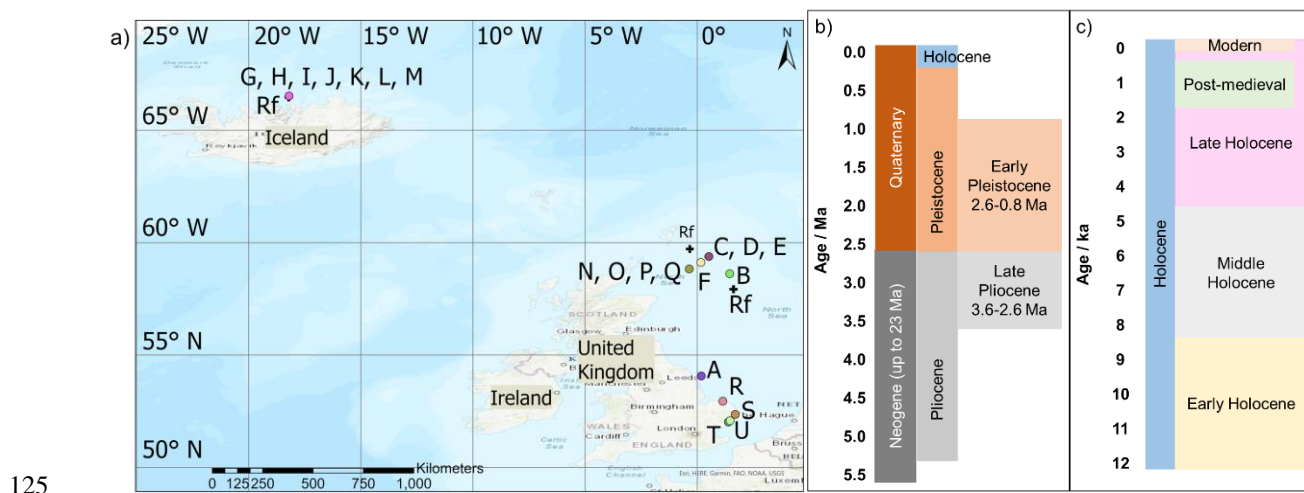
105 We present here a new method for the preparation of aragonitic *A. islandica* shells for AAG. To develop this
106 methodology, the following experiments were conducted:

- 107 - optimisation of the sampling method and isolation of the three microstructural layers (Sect. 2.2);
- 108 - assessment of aragonitic mineral diagenesis via X-ray diffraction (XRD) analysis (Sect. 3.1);
- 109 - testing for the existence of an intra-crystalline protein fraction via oxidation experiments (Sect. 3.2);
- 110 - testing for closed-system behaviour of *A. islandica* through controlled high temperature decomposition
111 experiments and assessment of the amino acid degradation patterns (Sect. 3.3);
- 112 - assessment of any change in amino acid composition and D/L values with ontogeny (Sect. 3.4);
- 113 - optimised method and recommendations for IcPD analysis of *A. islandica* (Sect. 3.5);
- 114 - analysis of multiple independently-dated subfossil shells to develop an initial AAG framework for *A. islandica*
115 in the North Atlantic Ocean (Sect. 3.6);
- 116 - age rangefinding of undated shells collected during research cruise DY150 of RRS *Discovery* in spring 2022
117 (Sect. 3.7).

118 2 Materials and methods

119 2.1 *A. islandica* specimens

120 In total, 19 *A. islandica* subfossil samples from the North Sea and Iceland were obtained for the bleaching and high
 121 temperature experiments, ontogenetic trends and initial framework; these spanned in age from modern to ~2.1-2.2 Ma
 122 and were independently dated with radiocarbon (^{14}C), AAG on other biominerals (see Table 1 for details; Fig. 2), and
 123 sclerochronological crossdating (S; Table 1). In addition, 160 *A. islandica* shells of unknown age, incorporating
 124 samples from both the North Sea and the North Icelandic shelf, were analysed for range-finding (Sect. 3.7; Fig. 2).



126 Figure 2. a) Location of the *A. islandica* samples analysed in this work. Map created using ArcGIS Pro. Geological
 127 timeline of the b) Pliocene and Pleistocene and Holocene on a million-year scale, and c) Holocene on a thousand-year
 128 scale (IUGS International Chronostratigraphic Chart, 2023).

129 Table 1. Overview of the *A. islandica* shells analysed in this study: numbers correspond to the location on the map (Fig.2) and Rf indicates shell
130 locations used in the rangefinding study (Sect. 3.7). Methods of dating: AAG: amino acid geochronology; ¹⁴C: radiocarbon; S:
131 sclerochronologically crossdated. * Note: beach-collected samples could range thousands of years in age (e.g. Dominguez et al., 2016). § Further
132 detail on radiocarbon dates are in Supplementary information Table S1. ※ Further information about sampling location is in Supplementary
133 information Table S2.

Sample name	Number of shells and code	Locality	Latitude	Longitude	Estimated age	Independent previous dating	Reference for previous dating	Experiment
A) ArBrMod	n=1 N/A	Bridlington beach, UK	54° 4' N	0° 11' W	Modern?*, beach collected July 2021	N/A	N/A	pXRD (Sect. 3.1), framework (Sect. 3.6), rangefinding (Sect. 3.7)
B) ArPe, ArPe2	n=2 N/A	North Sea off Peterhead	58° 37' N	1° 27' E	Modern, live-collected, trawled at - 114m depth in 2018	N/A	schnecken- und-muscheln.de (purchased in 2022)	Bleaching (Sect. 3.2), high temperature (Sect. 3.3), framework (Sect. 3.6), rangefinding (Sect. 3.7)
C) ArNsM1	n=1 0401381R	North Sea	59° 23.10' N	0° 31.00' E	1865-2004 CE	S	Butler et al., 2009	Ontogenetic trends (Sect. 3.4), framework (Sect. 3.6), rangefinding (Sect. 3.7)
D) ArNsM2	n=1 0401422L	North Sea	59° 23.10' N	0° 31.00' E	1874-2004 CE	S	Butler et al., 2009	Ontogenetic trends (Sect. 3.4), framework (Sect. 3.6), rangefinding (Sect. 3.7)
E) ArNsM3	n=1 0401423L	North Sea	59°23.10' N	0°31.00' E	1908-2004 CE	S	Butler et al., 2009	Ontogenetic trends (Sect. 3.4),

								framework (Sect. 3.6), rangefinding (Sect. 3.7)
F) ArNs0246	n=1 0400246	North Sea	59° 7.5' N	0° 10.0' E	1867-2004 CE	S	Butler et al., 2009	pXRD (Sect. 3.1), ontogenetic trends (Sect. 3.4), framework (Sect. 3.6), rangefinding (Sect. 3.7)
G) ArIcP2	n=1 061683M	Iceland	66° 31.59' N	18° 11.74' W	1397-1713 CE	S	Butler et al., 2013	Ontogenetic trends (Sect. 3.4), framework (Sect. 3.6), rangefinding (Sect. 3.7)
H) ArIcP1	n=1 061682M	Iceland	66° 31.59' N	18° 11.74' W	1171-1391 CE	S	Butler et al., 2013	pXRD (Sect. 3.1), ontogenetic trends (Sect. 3.4), framework (Sect. 3.6), rangefinding (Sect. 3.7)
I) ArIc617	n=1 061617	Iceland	66° 31.59' N	18° 11.74' W	2841±33 ¹⁴ C yr BP 2545-2119 cal yr BP 2σ	¹⁴ C §	n/a §	Framework (Sect. 3.6), rangefinding (Sect. 3.7)
J) ArIc711	n=1 061711	Iceland	66° 31.59' N	18° 11.74' W	2938±33 ¹⁴ C yr BP 2678-2292 cal yr BP 2σ	¹⁴ C §	n/a §	Framework (Sect. 3.6), rangefinding (Sect. 3.7)
K) ArIc407	n=1 061407	Iceland	66° 31.59' N	18° 11.74' W	3411±37 ¹⁴ C yr BP 3223-2817 cal yr BP 2σ	¹⁴ C §	n/a §	Framework (Sect. 3.6), rangefinding (Sect. 3.7)

L) ArIc746	n=1 061746	Iceland	66° 31.59' N	18° 11.74' W	3535±36 ¹⁴ C yr BP 3364-2975 cal yr BP 2σ	¹⁴ C §	n/a §	Framework (Sect. 3.6), rangefinding (Sect. 3.7)
M) ArIc305	n=1 061305	Iceland	66° 31.59' N	18° 11.74' W	4222±40 ¹⁴ C yr BP 4257-3826 cal yr BP 2σ	¹⁴ C §	n/a §	Framework (Sect. 3.6), rangefinding (Sect. 3.7)
N) ArNs0658	n=1 010658	Fladen Ground (North Sea)	58° 50' N	0° 21.35' W	7810±25 ¹⁴ C yr BP 8340-8100 cal yr BP 2σ	¹⁴ C (Marine13 calibration)	Estrella- Martinez, 2019	Framework (Sect. 3.6), rangefinding (Sect. 3.7)
O) ArNsP1	n=1 10660	Fladen Ground (North Sea)	58° 49.52' N	0° 21.6' W	7801±29 ¹⁴ C yr BP 8330-8070 cal yr BP 2σ	¹⁴ C (Marine13 calibration)	Estrella- Martinez, 2019	Ontogenetic trends (Sect. 3.4), framework (Sect. 3.6), rangefinding (Sect. 3.7)
P) ArNsP2	n=1 10682	Fladen Ground (North Sea)	58° 49.52' N	0° 21.6' W	7794±24 ¹⁴ C yr BP 8320-8060 cal yr BP 2σ	¹⁴ C (Marine13 calibration)	Estrella- Martinez, 2019	Ontogenetic trends (Sect. 3.4), framework (Sect. 3.6), rangefinding (Sect. 3.7)
Q) ArNsP3, ArNs0684	n=1 10684	Fladen Ground (North Sea)	58° 49.52' N	0° 21.6' W	7752±23 ¹⁴ C yr BP 8280-8020 cal yr BP 2σ	¹⁴ C (Marine13 calibration)	Estrella- Martinez, 2019	pXRD (Sect. 3.1), ontogenetic trends (Sect. 3.4), framework (Sect. 3.6), rangefinding (Sect. 3.7)
R) ArWey	n=1 N/A	Weybourne Crag, UK	52° 56.55' N	1° 08.33' E	Early Pleistocene (2.2-2.1 Ma)	AAG on <i>Bithynia</i> opercula and <i>Nucella</i> , biostratigraphic evidence	Preece et al., 2020	pXRD (Sect. 3.1), bleaching (Sect. 3.2), framework (Sect. 3.6)

S) ArEw	n=24 N/A	Easton Wood, UK	52° 21.43' N	1° 41.52' E	Early Pleistocene (2.35-2.25 Ma)	Biostratigraphic evidence	Mayhew, 2013	Framework (Sect. 3.6)
T) ArAh	n=6 N/A	Alderton House pit TM330415, UK	52° 1.2' N	1° 23.24' E	Late Pliocene, Early Pleistocene (3.6-2.12 Ma)	Lithological, biostratigraphic evidence	BGS; Hamblin et al., 1997	Framework (Sect. 3.6)
U) ArCg	n=3 N/A	Capel Green Pit TM376496, UK	52° 4.41' N	1° 27.5' E	Late Pliocene, Early Pleistocene (3.6-2.12 Ma)	Lithological, biostratigraphic evidence	BGS; Hamblin et al., 1997	Framework (Sect. 3.6)
Rangefinding Multiple names, see Table S2	n=73	Fladen Ground (North Sea)	Various ※	Various ※	Unknown	None	N/A	Rangefinding (Sect. 3.7)
Rangefinding Multiple names, see Table S2	n=87	North Icelandic shelf	Various ※	Various ※	Unknown	None	N/A	Rangefinding (Sect. 3.7)

2.2 Sampling

Each individual shell was sectioned from the umbo to the margin with an IsoMet 1000 precision cutter. After slicing, the shells were sonicated in deionised water ($18.2 \text{ M}\Omega \text{ cm}^{-1}$) until no residue was observed (3 min, 2-3 washes). After air drying, the periostracum (if present), was removed by drilling with an abrasive rotary burr on a hand-held rotary tool (Dremel drill). Each layer (oOSL, iOSL and ISL; Fig. 1), was sampled by drilling using a Dremel drill equipped with a stainless-steel diamond-coated drill bit with a small sphere or cylindrical tip. Following the experiments in sections 3.3 and 3.4, the iOSL layer was chosen for building the AAG framework. To check changes in amino acids with ontogeny (e.g. with the biological age of the shell; Sect. 3.4), the iOSL from early and late ontogeny within one shell (Table 1) was sampled: the former near the hinge and the latter close to the ventral margin of the shell, likely containing a few annual growth increments. To build the AAG framework (Sect. 3.7), intact Quaternary shells were subsampled near the margin of the shell where the iOSL was thickest. Fragmented shells were sampled where the iOSL was thickest, for ease of sampling. Between each sample the drill tip was cleaned in a 0.6 M HCl (Fisher, analytical grade) solution and MeOH (Fisher, HPLC grade) to reduce cross-contamination of samples.

2.3 Bleaching procedure

Following protocols developed by Penkman et al., (2008), approximately 20-30 mg of powder was transferred to a 2 mL plastic microcentrifuge tube (Eppendorf) and NaOCl (12 %, VWR, 50 uL mg^{-1} of sample) was added. Samples were oxidised for 24-72 h for bleaching experiments (Sect. 3.3). Following the results of these experiments, the iOSL layer of all other subfossil samples was oxidised for 48 h. After the allotted time, the NaOCl was removed, and the powder was washed six times with deionised water ($18.2 \text{ M}\Omega \text{ cm}^{-1}$) and once with MeOH (Fisher, HPLC grade). The samples were left to air dry for one to two days.

2.4 High temperature experiments

High temperature experiments were carried out in a BinderTM ED23 oven set to 140°C . To the bleached powder (10-20 mg), $300 \text{ }\mu\text{L}$ of deionised water ($18.2 \text{ M}\Omega \text{ cm}^{-1}$) was added in a glass vial (Penkman et al., 2008). The samples were exposed to high temperature conditions of 140°C for 8, 24 and 48 h. After this time, the water was carefully removed and the powder was left to air dry for 1-2 days.

2.5 Isolation of free (FAA) and total hydrolysable amino acids (THAA)

Following bleaching and in some cases high temperature exposure, the dry powder (1-10 mg) was split between free amino acids (FAA) and total hydrolysable amino acids (THAA; Penkman et al., 2008). The FAA were demineralised in 2 M HCl (10 uL mg⁻¹ of sample, minimum possible volume) and dried over a rotary vacuum concentrator (Christ RVC 2-25 CDplus, 1300 rpm). The THAA samples were hydrolyzed in 7 M HCl (20 uL mg⁻¹ of sample) and heated at 110 °C for 24 h to hydrolyse the peptide bonds. The samples were then dried in a rotary vacuum concentrator.

2.6 UHPLC-FLD analysis

Samples were rehydrated with a solution containing an internal standard - L-homo-arginine (0.01 mM), sodium azide (1.5 mM) and HCl (0.01 M) - to enable quantification of the amino acids. Analysis of chiral amino acid pairs was achieved using an Agilent 1200 Series HPLC fitted with an Agilent Eclipse Plus C₁₈ column (4.6 x 100 mm, 1.8 um particle size) and fluorescence detector (excitation wavelength = 230 nm, emission wavelength = 445 nm), using a UHPLC method modified from Crisp (2013; Table 2). The binary mobile phase consisted of: (A) sodium acetate buffer (23 mM sodium acetate trihydrate, sodium azide, 1.3 µM EDTA, adjusted to pH 6.00 ± 0.01 with 10% acetic acid and sodium hydroxide), and (B) 92.5:7.5 methanol:acetonitrile. Table 2 reports the mobile phase, flow rate and temperature gradient of the separation. Data processing was performed on ChemStation and data analysis on Excel; all data discussed in this paper is reported in Supplementary information, Table S2. The Crisp (2013) method, is able to separate the L and D enantiomers of 14 amino acids.

Table 2. Gradient of mobile phase, flow rate and column temperature for the UHPLC-FLD method. ‡ indicates that the parameter does not change at the referred timepoint.

Time / min	% A / sodium acetate buffer	% B / 92.5:7.5 methanol:acetonitrile	Flow rate / mL min ⁻¹	Column temperature / °C
0.0	90	10.0	1.25	25
8.8	82.0	18.0	1.25	‡
10	82.0	18.0	1.25	28
11	82.0	18.0	1.25	28
23	78.3	21.7	1.25	28
25	78.3	21.7	1.25	28

32	75.2	24.8	1.25	28
34.5	74.0	26.0	1.25	28
36	65.0	35.0	1.25	28
50	‡	‡	1.30	25
56	50.0	50.0	1.30	25
62	2.0	98.0	1.30	25
67	95.0	5.0	1.25	25

2.7 Powder XRD analysis

Powder X-ray diffraction analysis was carried out on a selection of samples (Table 1) using a Bruker Panalytical Aeris Powder XRD, scanned between 0-70° 2 θ using a 0.2-degree increment per second. The scan axis was Gonio, source filter was Beta nickel, beam mask was set to 20, beam knife to high, and antiscatter was 9 mm. The samples analysed were powdered either by a rotary burr on a drill (section 2.2) or by homogenising to a fine powder with an agate pestle and mortar. Homogenised *Cepea* spp. shells were used as aragonite standards and modern ostrich eggshell (OES) as calcite standard.

3 Results and discussion

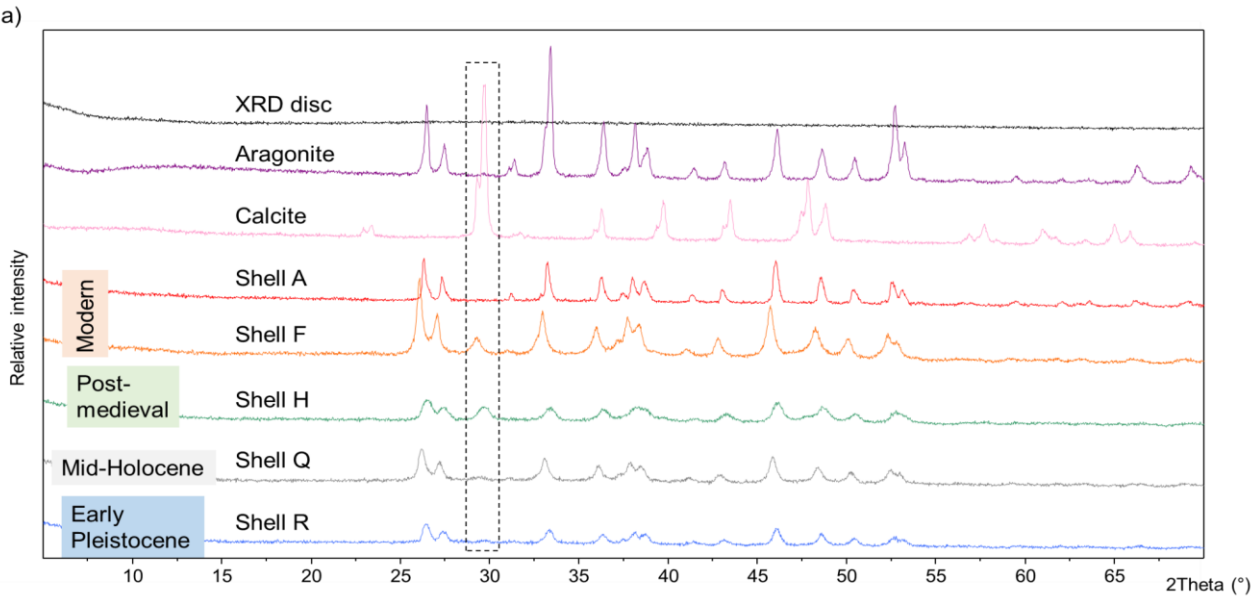
The multilayer nature of *A. islandica* (comprising the oOSL, iOSL and ISL; Fig. 1) means that there are likely to be protein differences between layers. This will dictate the original amino acid concentration and composition, and therefore their diagenesis, with impacts on D/L values and AAG. Initially we present an assessment of the mineralogy (Sect. 3.1), followed by the results from bleaching (Sect. 3.2) and heating experiments on the three microstructural layers (Sect. 3.3), assessing the amino acid composition, concentration and D/L values. Ontogenetic trends on modern and subfossil shells are presented in section 3.4. Recommendations for the method for AAG analysis of *A. islandica* (Sect. 3.5) are followed by an initial AAG framework over the Quaternary period (Sect. 3.6), and application of the method to age rangefinding undated shells (Sect. 3.7).

3.1 Assessment of sampling procedure and mineral diagenesis

Aragonite, the polymorph of CaCO₃ that makes up the three layers of the shells of *A. islandica*, can convert into calcite over geological timescales or under stress (Brand and Morrison, 1987). The transition state in the transformation of labile aragonite into calcite can have implications for the integrity of any closed system and the IcP (Preece and Penkman, 2005; Penkman,

2010). Thus, investigating the mineral composition of samples may help to identify compromised samples; this can be done using X-ray diffraction. In order to understand any potential changes to the CaCO_3 structure, powder XRD was carried out on a selection of samples of a variety of ages to qualitatively assess the presence of aragonite and/or calcite (Table 1).

The diffractograms of modern (shells A and F), post-medieval (shell H), Mid-Holocene (shell Q; Walker et al., 2019) and Early Pleistocene (shell R) shells that were drilled show a small peak of calcite (2θ 29°) in the mainly aragonitic shells (Fig. 3a). There is no clear pattern between the age of the sample and the presence or absence of calcite; the Early Pleistocene shell (shell R, 2.2-2.1 Ma) shows only a very small calcite peak, compared to larger peaks in the modern and post-medieval shells. Individual burial conditions will impact the potential for mineral diagenesis in a sample, but it is also possible that the abrasion and temperature created during the drilling process may affect the aragonitic crystal structure (Bäldreki et al., 2024). To test this, drilled powders were compared with shell chips from the same samples homogenised with a pestle and mortar (Fig. 3b). The chips do not show a calcite peak at 2θ 29° (Fig. 3b); these experiments indicate that any diagenetic calcite was below the limits of detection for these samples, and that the drilling process has caused some transformation of aragonite into calcite. However the drilling process is necessary in order to remove the periostracum and isolate and sample the required layers for AAG in this shell type. Other methods to remove the periostracum include using a scalpel, dipping the shell in HCl, NaOH or H_2O_2 (Checa, 2000; Agbaje et al., 2018), but it is challenging to isolate the individual mineralised layers without drilling. Therefore, it is important to use the lowest speed possible and avoid applying extreme pressure when sampling using a rotary drill.



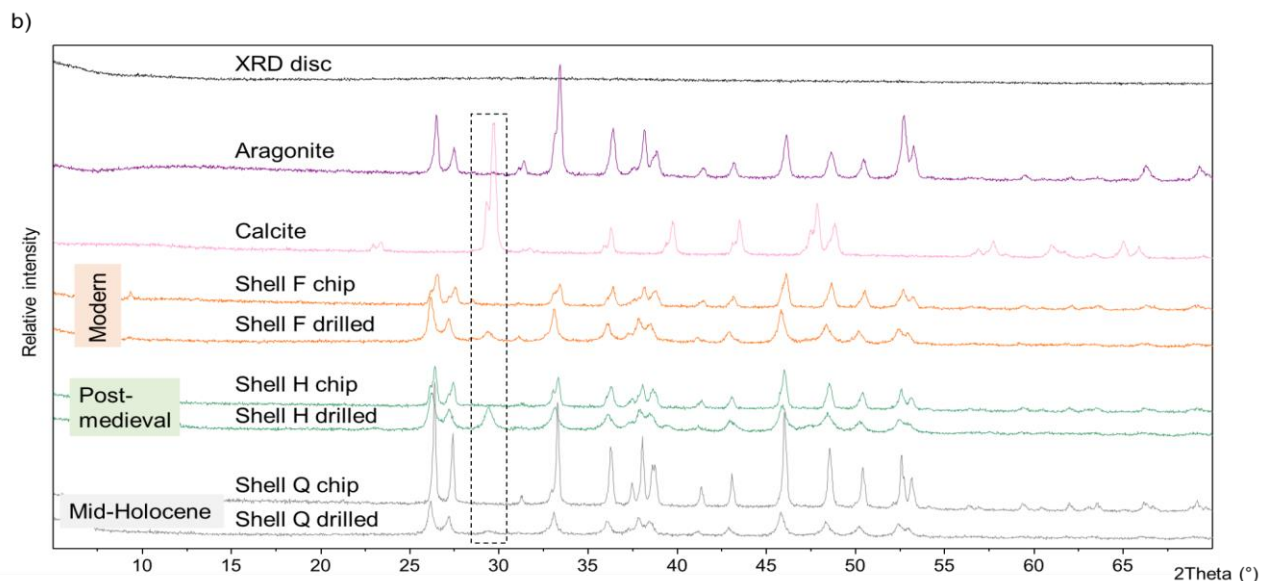


Figure 3. (a) pXRD spectra of *A. islandica* shells of various ages, powdered using a drill; (b) pXRD spectra of *A. islandica* shells: in each case the same shell was drilled with a rotary burr (“drilled”), and homogenised with pestle and mortar (“chip”). The dashed area in black represents the main peak of calcite at 2θ 29°. As the drilling process may convert aragonite into calcite, it must be undertaken with care.

3.2 The impact of bleaching on amino acids

To test for any presence of an intra-crystalline protein fraction, bleaching experiments on each of the layers of *A. islandica* in threesells (Table 1) was undertaken: two modern samples (shell A, beach-collected and shell B, trawled) and an Early Pleistocene sample (shell R).

In the modern samples, the concentration of FAA and THAA in all layers decreases with bleaching (Fig. 4), meaning that an inter-crystalline fraction is removed. There is an initial sharp decrease and a subsequent very small increase in concentration after 24 h in the oOSL layer of shell B, possibly indicating that the prolonged bleaching process is breaking some of the peptide bonds, increasing the concentration of amino acids from the intra-crystalline fraction. In the iOSL and ISL layers of shells A and B, the concentration reaches a plateau (i.e. little or no change in trend between two or more observations) between 48 and 72 h, indicating that an intra-crystalline fraction is more resistant to bleaching than the unbleached shells and therefore requires long oxidation exposure. This isolated intra-crystalline fraction represents $17 \pm 3\%$ (all errors represent 1σ around the mean) of the oOSL, $16 \pm 5\%$ of the iOSL and $15 \pm 2\%$ of the ISL in the unbleached FAA fraction of shell B. The total concentration in the FAA fraction is 1.5-2 orders of magnitude smaller than in the THAA fraction; as the sample is young there would have

233 been little natural breakage of the peptide bonds to form free amino acids. Following an initial drop in concentration from 0-
234 24 h, the concentration is stable in the THAA fraction with increasing bleaching time in all layers in both shells. This intra-
235 crystalline fraction represents $13 \pm 0.5\%$ of the oOSL ($\sigma=1$), $10 \pm 1\%$ of the iOSL ($\sigma=1$), and $15 \pm 1.5\%$ of the ISL in the total
236 unbleached THAA fraction for shell A. For shell B the bleached amino acids represent $7 \pm 0.1\%$ of the oOSL and the iOSL
237 ($\sigma=1$), and $18 \pm 1\%$ of the ISL. In summary, the FAA and THAA in the intra-crystalline fraction are stable and isolated
238 between 24-48 h of bleaching in the modern *A. islandica* shell.

239 The geological formation of free amino acids through peptide bond hydrolysis is evident in the Early Pleistocene shell from
240 Weybourne Crag (shell R; Fig. 5). Similarly to the modern sample, the Early Pleistocene FAA and THAA decrease in
241 concentration with bleaching; the variability between replicates is larger so identification of the plateau is more challenging,
242 potentially lying between 48 h and 72 h in both the THAA and FAA fractions. Sykes et al. (1995) noted that solid slices of
243 modern *A. islandica* were less susceptible to 10% NaOCl oxidation compared to the shell powder - in the latter aspartic acid
244 concentration reached a plateau after 10 h - indicating that the intra-crystalline fraction for the powdered shell was isolated
245 after just 10 h of oxidation. In our study, when the individual shell layers are isolated and powdered, a concentration plateau
246 is only achieved between 24 and 48 h (Fig. 5); in contrast to the results from Sykes et al. (1995), we therefore suggest that
247 bleaching for 48 hours is necessary to securely isolate the intra-crystalline protein fraction. In the Early Pleistocene shell, the
248 percentage of intra-crystalline fraction compared to the unbleached FAA fraction is $61 \pm 5\%$ in the oOSL, $38 \pm 5\%$ in the
249 iOSL, and $70 \pm 7\%$ in the ISL; for the THAA fraction the intra-crystalline fraction represents $49 \pm 5\%$ of the oOSL, $30 \pm 1\%$
250 of the iOSL, and $55 \pm 6\%$ of the ISL. Due to the age of the shell, it is not surprising that the majority of the FAA are intra-
251 crystalline, with the more labile inter-crystalline free amino acids likely to have leached out of the system (Sykes et al., 1995).
252 Despite the age of the shell (~2.2-2.1 Ma), there are both inter- and intra-crystalline amino acids present (Demarchi, 2009;
253 Penkman et al., 2011; Demarchi et al., 2013a-b; Ortiz et al., 2015, 2018). It is interesting to note that the ISL and oOSL layers
254 contain a higher relative percentage of intra-crystalline protein (oOSL = $49 \pm 5\%$, ISL = $55 \pm 6\%$), whereas the iOSL has a
255 much lower proportion of IcP ($30 \pm 1\%$).

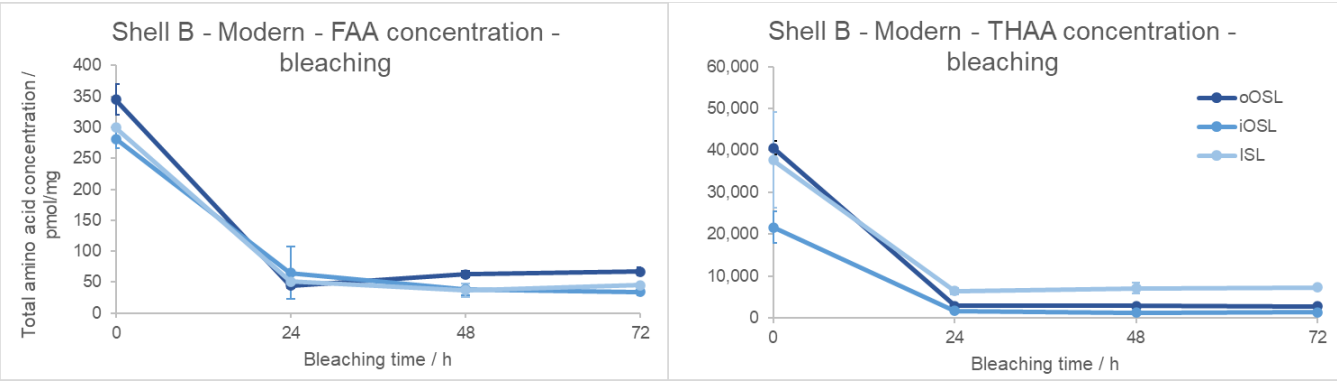
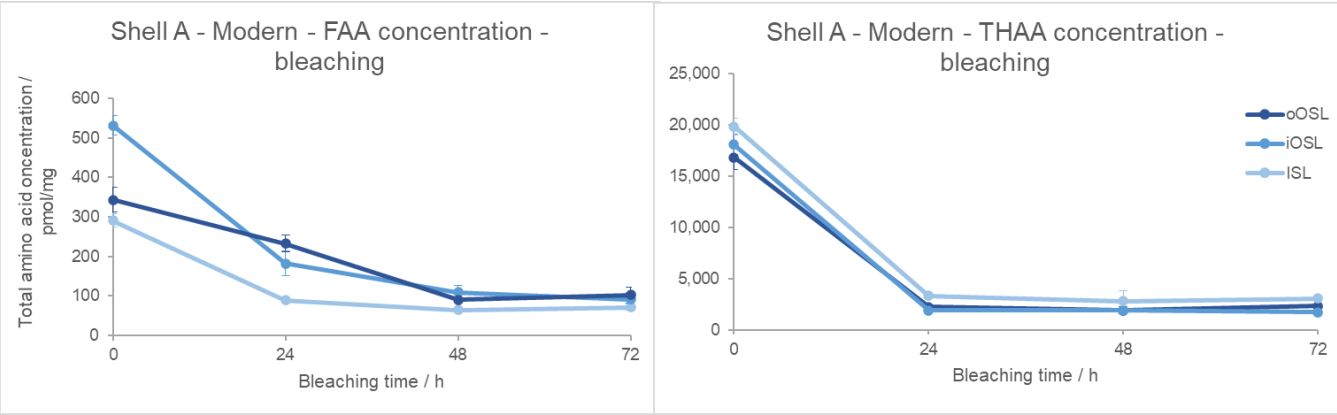


Figure 4. Decrease in total amino acid concentration upon bleaching modern *Arctica islandica* (shell A from Bridlington beach, UK, and B from the North Sea off Peterhead, UK) for the oOSL, iOSL and ISL microstructural layers. Error bars indicate one standard deviation about the mean based on two replicated (shell A) and three replicates (shell B). Note the large drop in concentration with bleaching, with a plateau reached by 48 h.

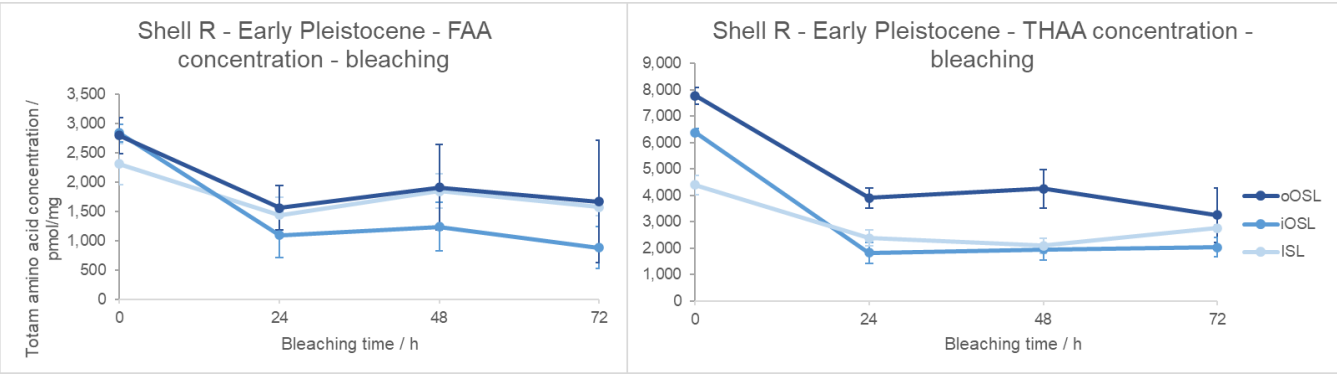


Figure 5. Change in total amino acid concentration upon bleaching Early Pleistocene *A. islandica* (shell R from Weybourne Crag, UK) for the oOSL, iOSL and ISL microstructural layers. Error bars indicate one standard deviation about the mean based on two replicates. Note the drop in concentration with bleaching with a plateau reached by 48 h within error bars.

As the oxidation step has been shown to induce some racemisation in other mollusc shells, especially with long exposure (Penkman et al., 2008), when choosing the optimal bleaching time both concentration and racemisation have to be considered. In the modern and Early Pleistocene samples there is an initial increase in D/L for Asx (aspartic acid), Glx (glutamic acid), Ser (serine), Ala (alanine) and Val (valine) between 0-24 h bleaching, indicating that the removal of the inter-crystalline protein leaves more racemised amino acids in the IcP (Penkman et al., 2008). The D/L values reach a plateau between 24 h and 48 h, and at the 72 h timepoint the D/L values slightly increase for most amino acids, suggesting that some oxidation-induced racemisation is taking place (Fig. 6). Nevertheless, the concentration plateau reached at 48 h in both the modern and Early Pleistocene samples and the small change in D/L values indicates that the intra-crystalline protein fraction is effectively stable and relatively protected from oxidation.

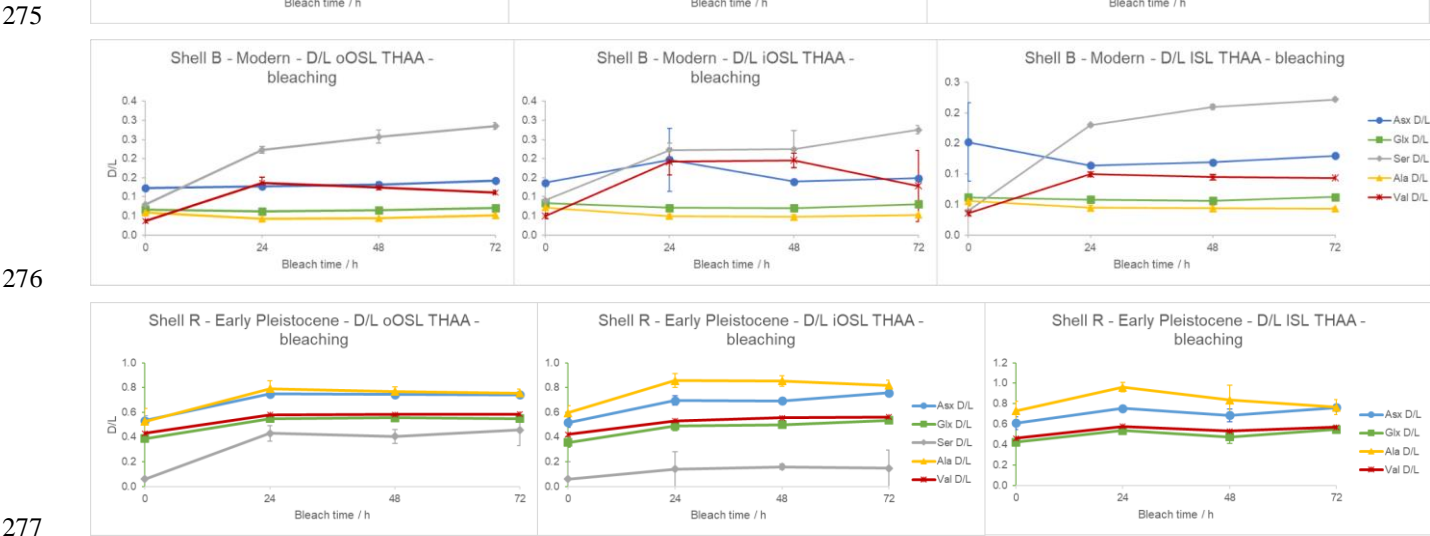


Figure 6. Mean THAA D/L of Asx, Glx, Ser, Ala & Val in *A. islandica* upon bleaching for the oOSL, iOSL and ISL microstructural layers. Top: modern shell from Bridlington beach (shell A); error bars indicate one standard deviation based

on three replicates. Middle: modern shell from the North Sea (shell B); error bars indicate one standard deviation based on three replicates. Bottom: Early Pleistocene shell from Weybourne Crag (shell R); error bars indicate one standard deviation based on two replicates. There is an initial increase in D/L with bleaching, but stable D/L with prolonged bleaching.

The percentage composition of each amino acid in the bleached and unbleached samples can provide information about the nature of protein in the two fractions, if different. The composition of the unbleached shell and IcP is similar for the THAA fraction, but some differences are present in the FAA fraction in the modern sample (Fig. 7, Supplementary information Fig. S1). In this fraction, in the bleached samples of shell B, Gly (glycine) is much higher and Ser, Ala and Arg (arginine) are lower; however, this may be due to the very low concentrations of minor amino acids, sometimes below the limit of detection. In the Early Pleistocene sample, the composition is very similar between the unbleached and bleached fractions in both the FAA and THAA (Supplementary information Fig. S2), confirming that the majority of amino acids in the unbleached samples are intra-crystalline, and that much of the inter-crystalline protein fraction has leached out with time.

In addition to differences in amino acid concentration between the three layers of *A. islandica*, there are also slight differences in composition between layers. In the THAA fraction of the modern shells bleached for 48 h, all three layers have similar composition, with some exceptions: Ala is higher in the iOSL and Arg is lower in the ISL than in the other two layers for shell B. Shell A shows slightly lower composition of Asx and Glx in the oOSL compared to the other two layers and also shell B, however the variability between samples is larger for these amino acids in shell A than shell B, complicating interpretation. The percentage composition of Gly is slightly higher in the oOSL than the iOSL and ISL for both shells A and B, although the between-sample variability is larger than for the other two layers which may confound the results for shell B (Fig. 7). In the Early Pleistocene shell, the FAA fraction shows very similar composition between the three layers. In the THAA fraction, the ISL and iOSL contain higher amounts of Asx and Glx, while Thr (threonine) is more abundant in the two OSL layers and Gly is highest in the ISL layer. There is mostly agreement in the composition of the two shells. The higher percentage composition of Gly in the Early Pleistocene shell is likely to be due to the natural diagenesis of Val (valine), Ser, Thr and Tyr (tyrosine) to form Gly (Vallentyne, 1964). Ser is much lower and Ala higher in the Early Pleistocene samples: Ser is thermally unstable and can degrade to form Ala and Gly (Vallentyne, 1964; Bada et al., 1978), while Ala can be a product of dehydration of Ser and Asx (Walton, 1998). The overall differences in amino acid composition in both modern and Early Pleistocene shells for the three layers shows that originally there are different proteins in the layers, which then break down at different rates; therefore, it is important to consistently sample one layer for reliable AAG.

Haugen and Sejrup (1990) presented the percentage composition of 30 modern unbleached specimens of *A. islandica* for both the inner and outer shell layers; as there was no separation into oOSL and iOSL, their results for the ‘outer’ layer are compared to our oOSL and iOSL results (Supplementary information Fig. S1b). Additionally, Haugen and Sejrup (1990) analysed their

310 amino acid with ion-exchange chromatography rather than HPLC, and they do not report His (histidine), Arg and Met
311 (methionine). The percentage composition of the FAA and THAA fractions from the modern shell B analysed here and the
312 30 shells from Haugen and Sejrup (1990) are very similar, with only small variations (Supplementary information Fig. S1b).
313 In the FAA fraction there is a lower contribution from Tyr in our data (3-4%) compared to 13-15% in the Haugen and Sejrup
314 (1990) shells, while Gly is higher in our data for the bleached shells (44-67%), but more comparable in the unbleached samples
315 (our work = 31-34%, Haugen and Sejrup, 1990 = 21-24%). In the THAA fraction the percentage composition from Haugen
316 and Sejrup (1990) are within error with our bleached data, while our unbleached shell has higher Gly and lower Asx and Glx.
317 There is remarkable similarity in percentage composition between Haugen and Sejrup (1990) results without bleaching and
318 our modern bleached shells; this may ultimately enable the comparison between data from samples analysed prior to and after
319 establishing the bleaching step in the AAG method.

320 A recent study compared the percentage composition of amino acids in untreated and oxidised modern shells, including 12%
321 NaOCl treatment on powdered shell where the layers had been homogenised (Huang et al., 2023). Similar to our results, Gly,
322 Asx and Glx were the dominant amino acids in the unbleached shells, followed by Ala, Ser and Thr (Supplementary
323 information Fig. S1a). Upon bleaching, Pro (proline) was the most abundant amino acid (Huang et al., 2023), but this
324 secondary amino acid is not quantified in the current analytical method used for AAG. As in our bleaching experiments, in
325 the work of Huang et al. (2023) upon bleaching Gly decreased in composition, while Asx, Glx, Ala, Val, Arg, Phe showed an
326 increase in composition; other amino acids present in lower concentrations show no or opposite trend. There is therefore a
327 general agreement between the study from Huang et al. (2023) and our current work, with the differences possibly due to the
328 sampling approach: Huang et al. (2023) homogenised all three aragonitic layers after removing the periostracum, whereas our
329 study separates the oOSL, iOSL and ISL, providing a more detailed study of the amino acid composition in the three
330 microstructural layers.

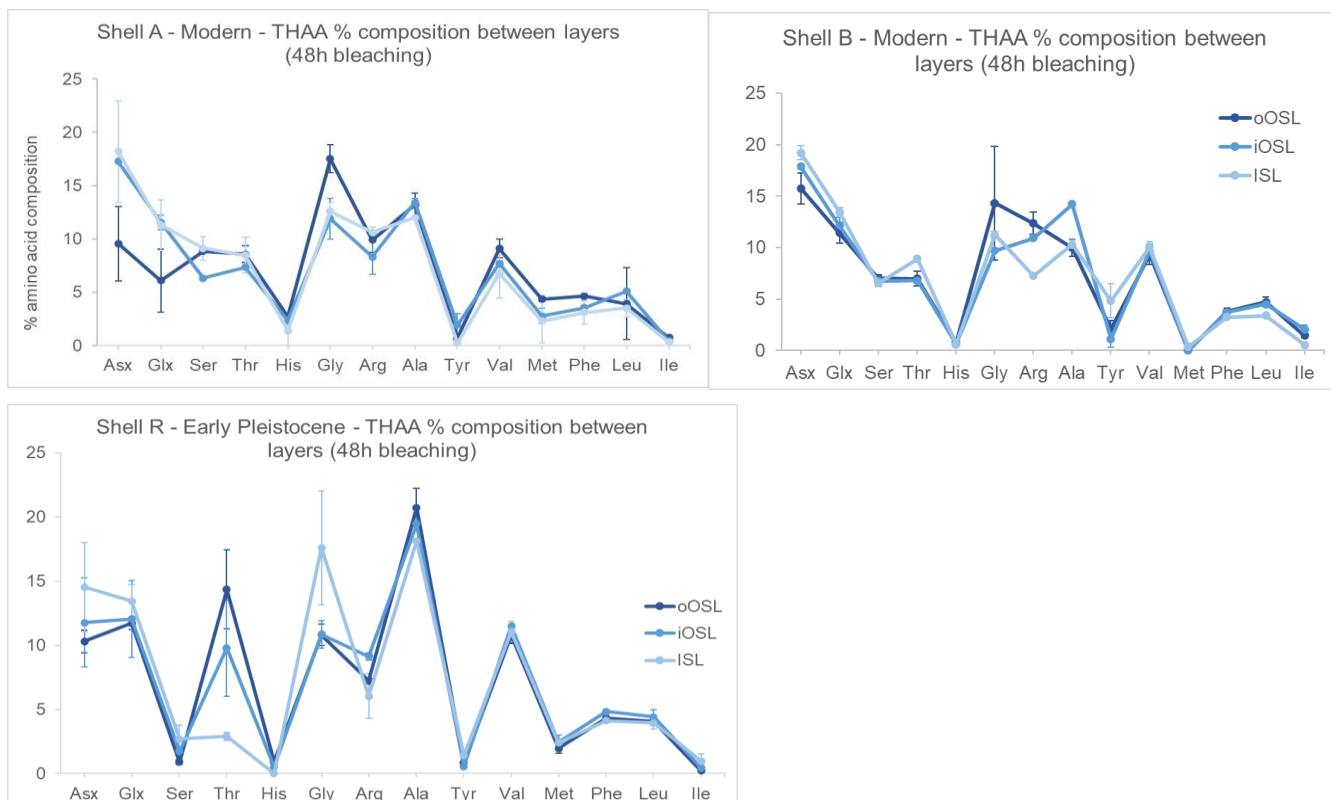


Figure 7. Mean THAA percentage composition after 48 hours of bleaching in the three microstructural layers of *A. islandica* from modern samples (shell A from Bridlington, and shell B from the North Sea), and from an Early Pleistocene sample (shell R). Error bars represent one standard deviation based on three replicates for shell B, and two replicates for shells A and R. There are differences in amino acid composition between the three aragonitic layers in the modern and Early Pleistocene shells, indicating differences in original protein composition.

3.3 Elevated temperature experiments to test for closed system behaviour

High temperature experiments are considered a controlled, simple way to assess the suitability of biomineral proteins for AAG (Kriausakul and Mitterer, 1978; Haugen and Sejrup, 1992; Penkman et al., 2008; Hendy et al., 2012; Demarchi et al., 2013). The resistance of the IcP to oxidation was shown with bleaching experiments on modern and Pleistocene shells (Sec 3.2). To test whether the IcP behaves like a closed system, the bleached powder (48 h) from the three layers of modern *A. islandica* shell B (Table 1) was exposed to high temperatures in hydrous conditions (140°C for 8, 24, 48 h), and the protein degradation (including rates of racemisation) observed. The high temperature experiments are utilised to accelerate the protein degradation and explore the processes that would otherwise occur over thousands of years. Previous studies showed that the degradation

patterns in high temperature heating experiments do not necessarily produce the same degradation patterns in subfossil samples; low temperature treatment (~80°C) may be more similar to subfossil results but requires long exposure (Crisp et al., 2013; Tomiak et al., 2013; Demarchi et al., 2013). Nevertheless, the chosen temperature of 140°C allows for quick assessment of protein degradation patterns and leaching over short timescale (a few days), while trends in concentration and D/L values, and correlations of FAA and THAA D/L with increased exposure to 140°C can provide evidence on whether the amino acids in *A. islandica* behave as a closed-system (Penkman et al., 2008).

The total concentration of FAA in the intra-crystalline fraction increases over time because prolonged heating breaks the peptide bonds to ultimately release free amino acids (Fig. 8). The total THAA concentration decreases with heating due to the decomposition of amino acids (Penkman et al., 2008; Crisp et al., 2013; Tomiak et al., 2013; Demarchi et al., 2013), discussed in detail below. An interesting observation is that the ISL layer has a higher THAA concentration than the other layers, but also has a steep increase in FAA concentration with heating time, coinciding with a steep drop in THAA concentration. This means that the amino acids in the inner layer (ISL) are more susceptible to peptide bond hydrolysis, and in the hydrolysable fraction (which includes both bound and free AAs), they are more prone to decomposition than the outer layer. This may be due to differences in the proteins' primary sequence or higher structures, or a result of the way the proteins are mineral-bound in the ISL microstructure. Conversely, the concentration of FAA and THAA in the iOSL layer shows the least change, indicating that the protein in this layer may be more resistant to degradation.

The different rates of breakdown of the three layers indicate the importance of consistently sampling one microstructure for obtaining more reliable AAG results.

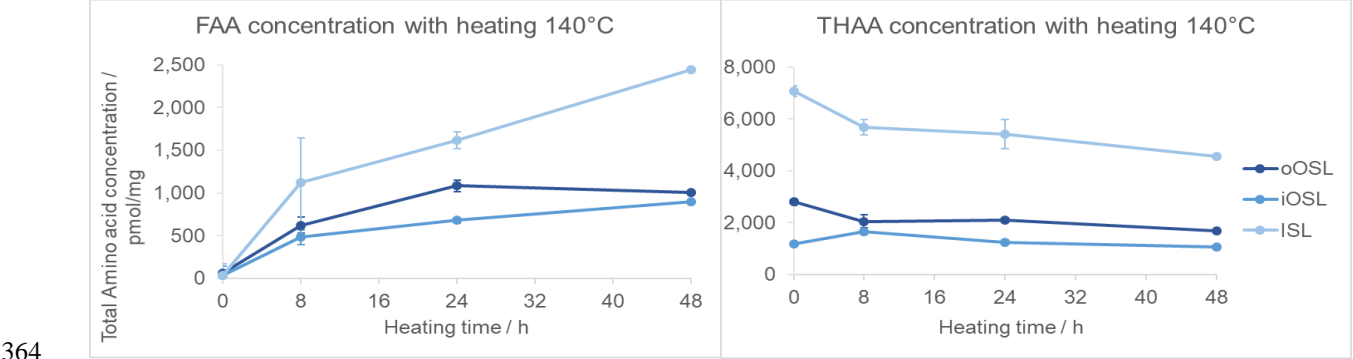


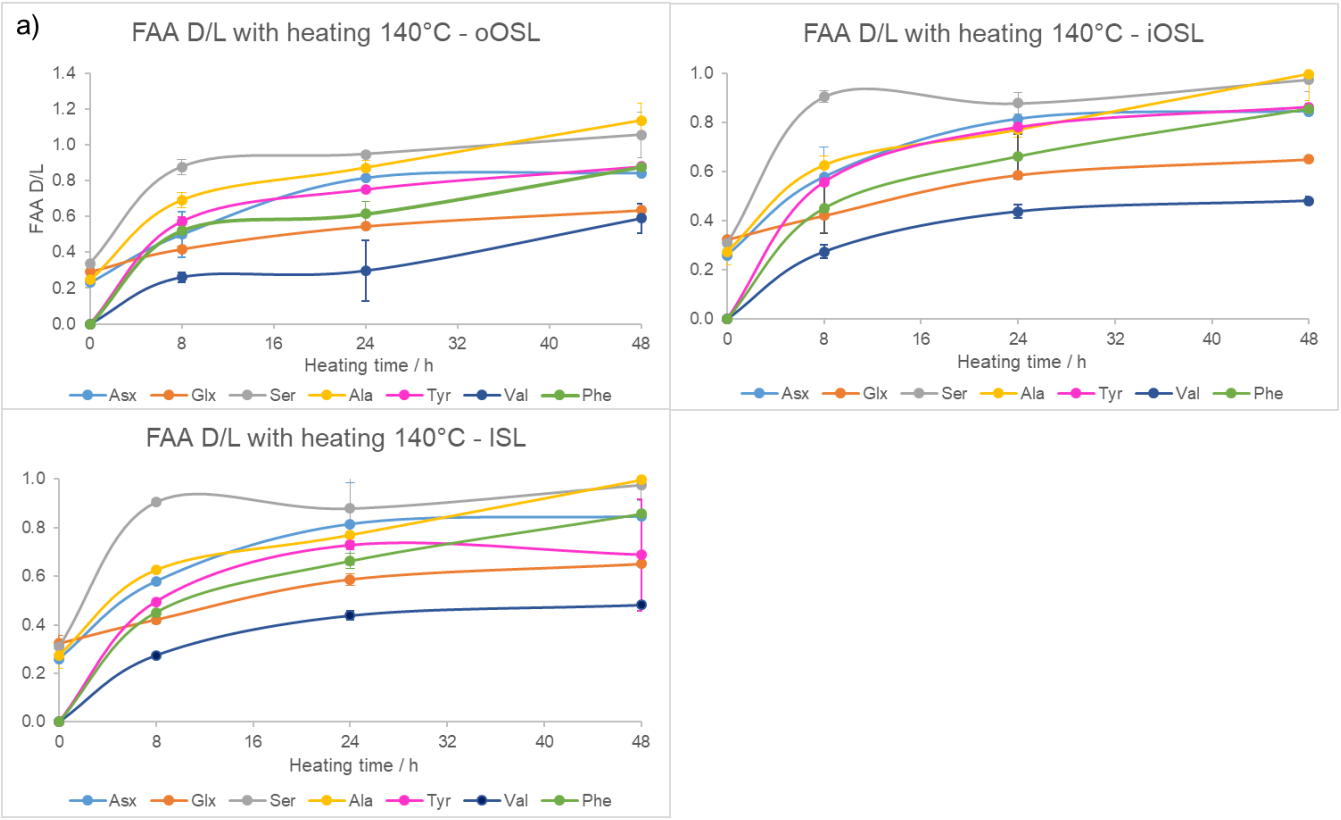
Figure 8. FAA and THAA concentration changes with heating at 140°C in the three shell layers of modern *A. islandica* shell B. Error bars indicate one standard deviation based on three replicates. The FAA concentration increases with heating due to peptide bond hydrolysis; the ISL seems to have faster peptide bond hydrolysis compared to the other layers.

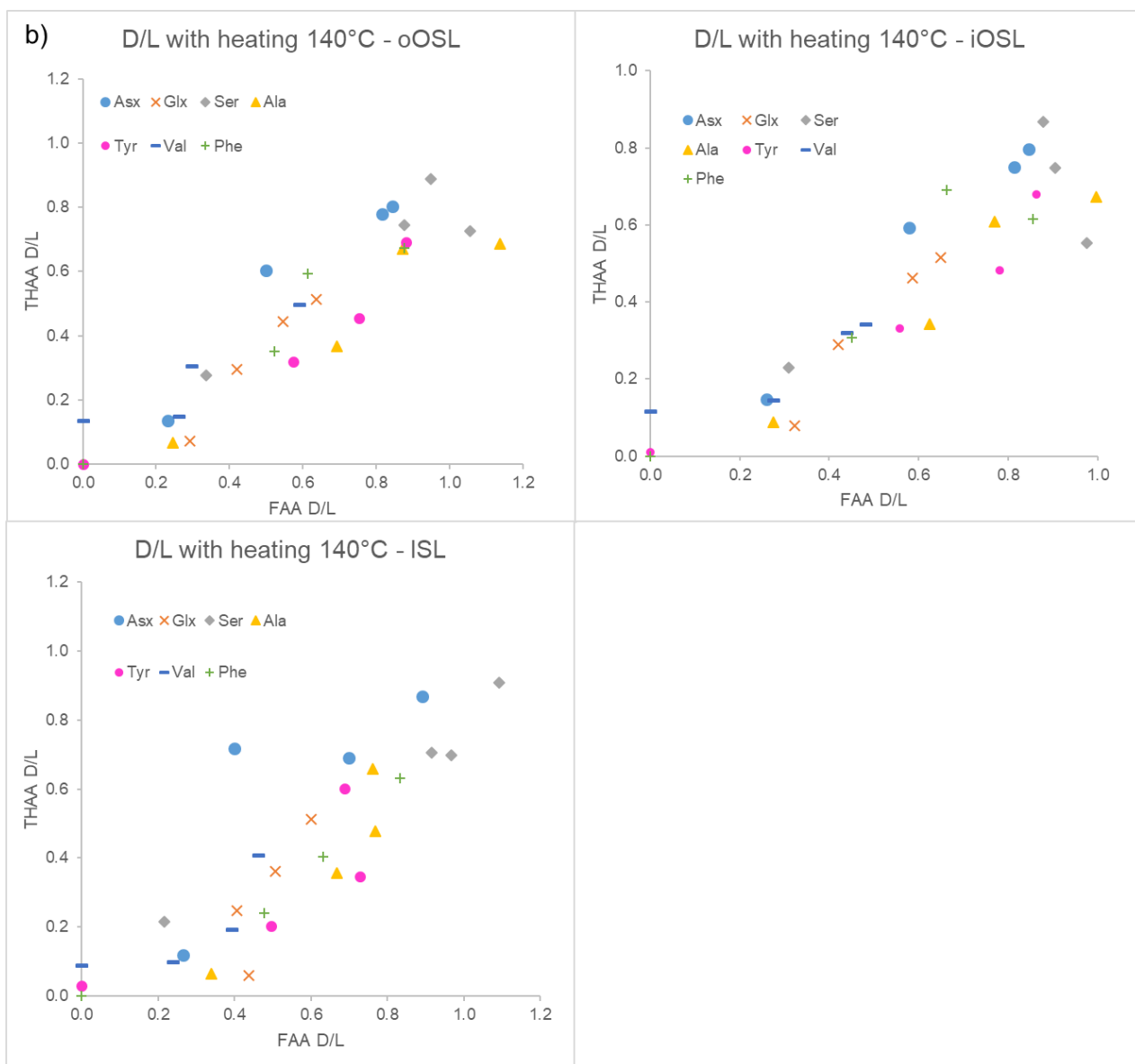
368 If *A. islandica* resembles a closed system the diagenetic products of protein degradation would be retained, and thus the FAA
369 and THAA D/L would be highly correlated (Preece and Penkman, 2005; Penkman et al., 2007; Demarchi et al., 2011, 2015.
370 As expected, the D/L values for all amino acids increase with increased heating duration in all layers (Fig. 9a, Supplementary
371 information Fig. S3) meaning that racemisation patterns follow reliable trends in the intra-crystalline protein fraction in *A.*
372 *islandica*. Figure 9b shows the correlation of FAA and THAA for Asx, Glx, Ser, Ala, Tyr, Val and Phe: overall, all amino
373 acids from all layers show high covariance indicative of closed-system behaviour. However, some scattering is observed for
374 the ISL layer. There is also some scattering for Ser especially in the outer layers, which is expected in these high temperature
375 experiments (Bright and Kaufman, 2011; Crisp et al., 2013) because the thermally unstable Ser (the “parent”) readily degrades
376 into Gly and Ala (the “products”). It is expected that the ratio of the “parent” over a degraded product will decrease with
377 heating and thus indicate increased decomposition (Bada et al., 1978). This is particularly evident after 8 h heating with a
378 marked reduction in the ratio of [Ser]/[Ala] (Fig. 10). In the THAA fraction Ser D/L decreases after 24 h (Supplementary
379 information Fig. S4) due to decomposition of free serine, resulting in a decrease in the overall racemisation of Ser (Penkman,
380 2010).

381 Other decomposition pathways include the degradation of Ser, Thr and Tyr (the “parent”) into Gly (Vallentyne, 1964), and
382 Asx (the “parent”) into Ala (Walton, 1998). These trends were observed in all cases in the FAA and THAA samples of the
383 iOSL layer after 8 h and in the oOSL layer after 24 h, whereas in the ISL layer the ratios increased in some cases
384 (Supplementary information Fig. S4). As previously mentioned for the concentration and D/L values, this could either be due
385 to how the different peptides are bound to the mineral, or differences in protein sequence and structure in the ISL layer
386 compared to the outer layers. Upon heating, the concentration of FAA increases at a high rate in the ISL (Fig. 8) and the steep
387 “parent”-product ratios may reflect the more labile nature of the peptide bonds. The THAA composition of the bleached
388 unheated ISL layer also shows a higher percentage of the more labile “parent” amino acids Asx, Thr and Tyr compared to the
389 outer layers, while Ser has similar composition in all three layers (Supplementary information Fig. S5). Therefore, the high
390 proportion of amino acids with labile peptide bonds in the ISL explains the high decomposition rate of FAA (Fig. 8) and the
391 faster degradation rates.

392 The high correlation between FAA and THAA amino acid D/L values and the predictable degradation pattern observed from
393 the high temperature experiments point towards a closed-system behaviour for *A. islandica* in all three layers. However, these
394 differences in rates of degradation between the inner and outer layers would affect the D/L values and the accuracy of the AAG
395 interpretation, therefore it is preferable to analyse one specific layer. Interestingly, in the ISL a high proportion of amino acid
396 is lost to hydrolysis in the THAA fraction and to degradation in the FAA fraction. In isotope studies the oOSL is not used
397 because it can be more readily contaminated or impacted by environmental factors, it being the most external layer (Schöne,
398 2013). The iOSL is routinely used in isotope analyses and can be used in sclerochronology (Schöne and Huang, 2021; Butler

et al., 2009). Due to the previous research on the iOSL, our bleaching and high temperature degradation experiments and ease of sampling the iOSL, we therefore suggest using this same layer for AAG.





402

403 Figure 9. (a) Mean FAA D/L with increased duration of heating at 140°C in the three bleached layers of modern *A. islandica* (shell
 404 B); error bars indicate one standard deviation based on three replicates. (b) FAA vs. THAA D/L with heating at 140°C. D/L values
 405 increase with increasing exposure to high temperature in all three aragonitic layers, and high correlation between the FAA and
 406 THAA fractions in most cases.

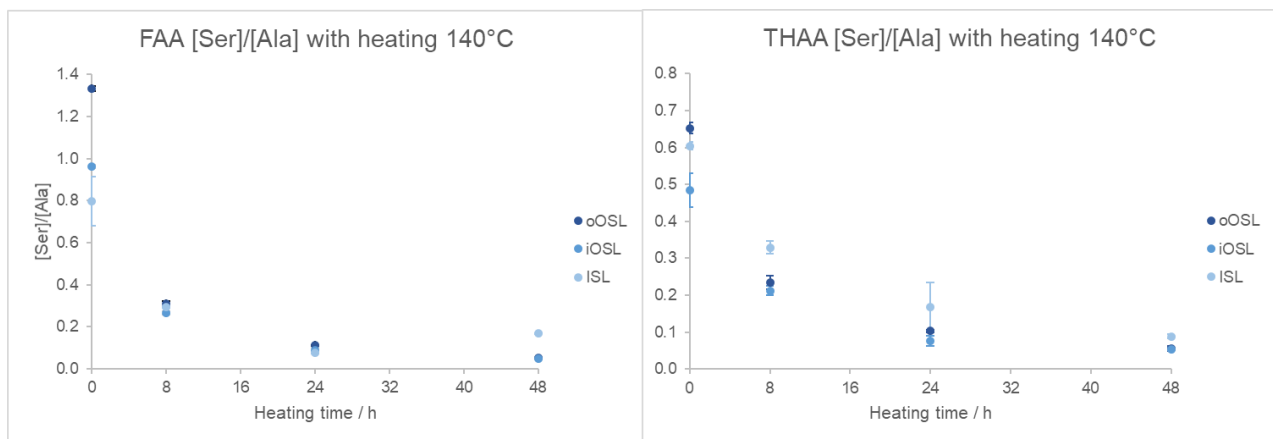


Figure 10. [Ser]/[Ala] in the bleached oOSL, iOSL and ISL layers of modern *A. islandica* (shell B) following heating at 140°C for 8-48 h. Error bars indicate one standard deviation based on three replicates. The [Ser]/[Ala] decreases with heating in all three aragonitic layers.

3.4 Assessing ontogenetic trends in modern and subfossil AAG

Previous work on amino acid $\delta^{15}\text{N}$ of *A. islandica* has shown changes in isotope values and amino acid composition with ontogeny, i.e. with biological age of the shell (Schöne and Huang, 2021). Here, the iOSL of eight shells with a known lifetime spanning 100-400 years (Table 1) were sampled near the hinge (representing the early ontogenetic age of the shell) and near the margin (representing late ontogeny), to check for any differences in composition and D/L values. Given the importance of original protein composition to the subsequent degradation, it is important to determine whether there are differences in concentration and D/L between early and late ontogeny as seen in amino acid isotopic analyses (Schöne and Huang, 2021). In addition, if the rates of the reactions are fast enough, it may be possible to use AAG for age resolution *within* an individual shell. For example, AAG has been used in sclerochronological studies of tropical *Porites* corals (e.g. Goodfriend et al., 1992), providing a resolution of ± 6 years in most recent material and ± 24 years in the last 150 years (Hendy et al., 2012). In these cases the ability to obtain high resolution data was due to the relatively high ambient temperatures ($\sim 26^\circ\text{C}$; Hendy et al., 2012) in which the corals live, but the lower temperatures of *A. islandica*'s habitat ($\sim 1\text{-}16^\circ\text{C}$; Schöne, 2013) mean that AAG for sclerochronology may not be applicable to this biomineral.

It is expected that the iOSL of samples from early ontogeny will have higher D/L values, because this part of the biomineral would have been deposited earlier in time; late ontogenetic samples will have lower D/L values. As the fastest racemising amino acids (Fig. 9a; Supplementary information Fig. S3), Asx, Ser and Ala were examined in detail (Fig. 11). The error bars are quite large in the FAA samples, likely due to the low concentrations of amino acids, so the data should be treated with

caution and therefore only the THAA are going to be discussed here. In the Mid-Holocene samples the D/L values for Asx, Ser and Ala show higher values in late ontogeny, contrary to the expectation (Fig. 11a). The intra-shell variability is very low ($\sigma=0.005-0.02$ for FAA and THAA), and the lack of ontogenetic trend is likely related to the older age of the shells confounding the *in vivo* degradation. The post-medieval shells do not show any significant ontogenetic pattern (Fig. 11b). The expected higher D/L values in early ontogeny are present in the modern shells FAA Asx, THAA Asx and Ser D/L plots, but not for Ala (Fig. 11c). Similarly to our data, Goodfriend and Weidman (2001) showed a gradual decrease in D/L in the unbleached outer layer of modern *A. islandica* shells from the umbo to the rim, but the trend was less evident in subfossil shells, especially in increments older than 1050 ± 35 (^{14}C age). The increments in early ontogeny also showed a much higher extent of racemisation connected with fast growth and large band ages compared to the rest of the shell, indicating that there are different proteins responsible for shell growth in early and late ontogeny (Goodfriend and Weidman, 2001). As a result, they recommended consistent sampling of the iOSL layer in late ontogeny or at least after increment year 20 (Goodfriend and Weidman, 2001).

It is notable that the D/L values in the THAA fraction of modern samples in early ontogeny follow the year of birth in the THAA fraction (Fig. 11c): meaning that the oldest shell that settled from larva first in 1865 has the highest D/L (Fig. 11b, shell C, blue circle), followed by the shell represented by the orange circle (Fig. 11b, shell D) which settled in 1874 and the least racemised sample is the shell that settled in 1908 (Fig. 11b, shell E, grey circle). For the post-medieval shells, intra-shell variation is high, especially for the D/L values corresponding to ~ 1400 CE. Similarly, the late ontogeny modern shells (Fig. 11c, shell C, D, E) all died in 2004 and should have similar D/L values, but they show great variability and/or large error bars, except for the FAA Asx D/L values.

The concentration of amino acids is higher in early ontogeny samples in the Mid-Holocene shells from the North Sea, whereas the opposite trend is observed in the post-medieval and modern shells (Supplementary information Fig. S6). Goodfriend and Weidman (2001) observed a slight decrease in percentage composition of Ser, Tyr, Met, Ile and Leu with age and an increase in Glu, Val, Ala and Asp with age. Overall, there is no specific trend in composition with ontogeny in our shells, although some of the palaeontological and modern shells show similar results to Goodfriend and Weidman (2001), indicating that there may be more acidic intra-crystalline proteins responsible for growth during early ontogeny compared to late ontogeny, where basic amino acids are more prominent (Supplementary information, Fig. S6). The different proteins in early and late ontogeny may also be responsible for the variability in D/L. In summary, the D/L values in early and late ontogeny of modern, post-medieval and Mid-Holocene age have high intra-shell and inter-shell variability, suggesting that AAG is not suitable for providing *within*-shell chronologies in *A. islandica* shells. Given the possible variability in D/L values and protein composition with ontogeny, it is recommended to consistently sample the iOSL layer for AAG; late ontogeny is preferred because of the increased thickness of the iOSL layer.

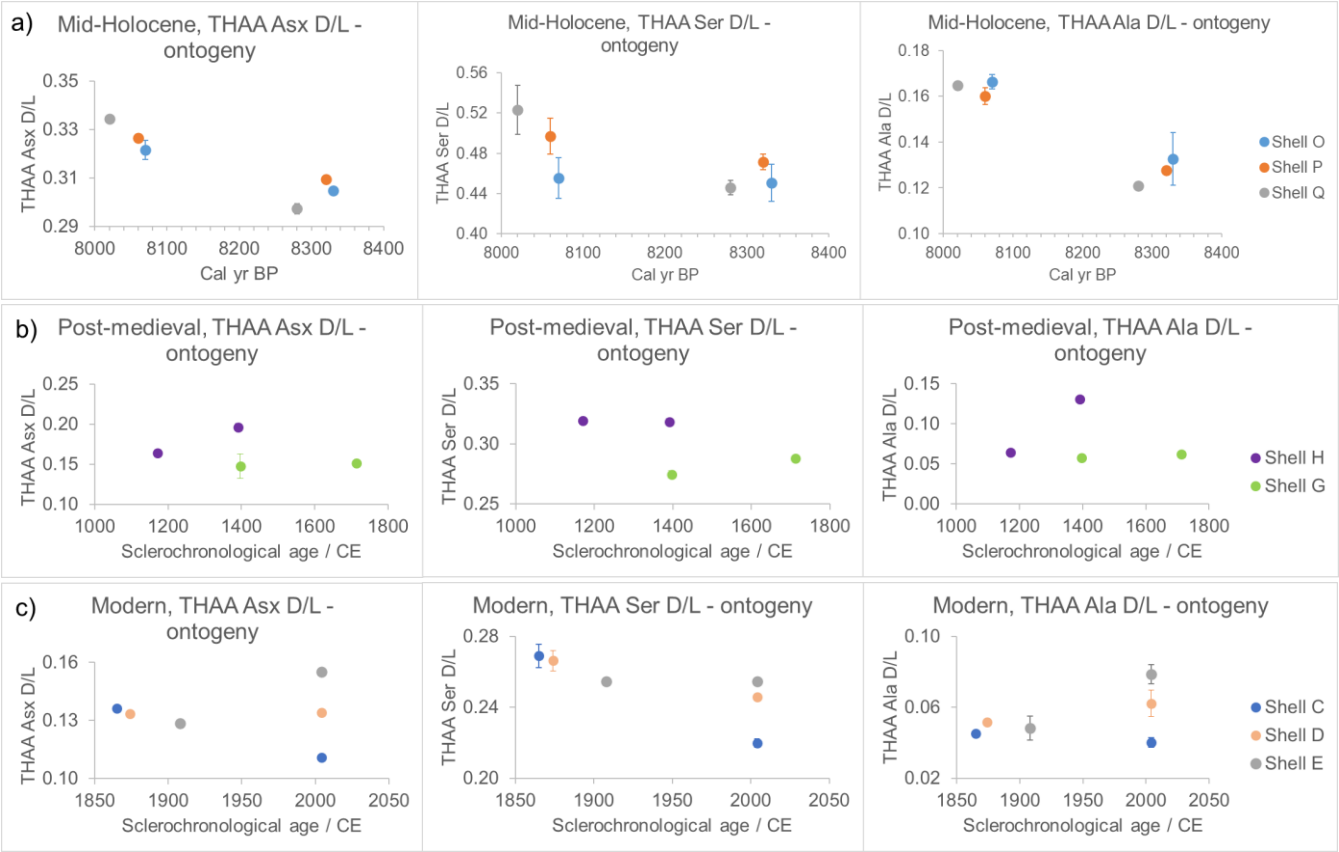


Figure 11. THAA Asx, Ser and Ala D/L for (a) Mid-Holocene (shells O, P, Q), (b) post-medieval (shells G, H), (c) modern *A. islandica* (shells C, D, E) early and late ontogeny samples. Note: the age of Mid-Holocene samples was assigned with radiocarbon dating, while for post-medieval and modern shells the age is based on sclerochronological cross-dating. The age sampled for AAG may vary slightly from the sclerochronological age reported. Error bars indicate one standard deviation based on two analytical replicates. Except for the modern samples, AAG shows no ontogenetic trends.

3.5 Optimised method and recommendations

The bleaching experiments have shown that the IcP of all three microstructural layers can be isolated after 48 h of bleaching (Figs. 4-5; Sect. 3.2). Heating experiments showed that all layers behave as a closed system. The ISL has a higher rate of peptide bond hydrolysis (Fig. 8), likely due to the higher percentage composition of labile amino acids compared to the outer layers. The slightly higher scattering in D/L values in the ISL (Fig. 9b) suggests the use of the outer shell layer for future dating. The low peptide bond hydrolysis and co-variance between FAA and THAA in the oOSL and iOSL suggests that these layers may provide more reliable dating (Sect. 3.3). Given that the iOSL is easier for sampling, as this layer is the widest, and

is already used in sclerochronological and isotope studies, we recommend using this layer for AAG. From the ontogenetic trends observed (Sect. 3.4), it is recommended to sample the late ontogeny (near the margin) portion of the iOSL; this should ensure more consistent protein analysis.

In conclusion, for AAG analysis of *A. islandica* we recommend cleaning of the shell in deionised water with sonication and selective drilling of the iOSL from a portion deposited in late ontogeny. The drilling step can be done by slicing the shell from the umbo to the margin (Sect. 2.2), and then either selectively drilling the iOSL with a hand-held rotary burr if this layer is thick, or drilling the oOSL away until the iOSL is reached and collecting only the latter layer. Caution needs to be taken to continuously move the rotary burr to reduce the build-up of temperature that can degrade the protein (Sect. 3.1). The powdered iOSL is then exposed to NaOCl for 48h and removed by washing with water and MeOH. The demineralisation, hydrolysis and UHPLC analysis steps are outlined in section 2.

3.6 An initial IcPD AAG framework for *A. islandica*

Following the isolation of a stable intra-crystalline protein fraction that shows effectively closed-system behaviour in the iOSL of *A. islandica* in laboratory experiments, we analysed subfossil shells with independent evidence of age to observe the amino acids' degradation patterns in *A. islandica* during the Quaternary and Late Pliocene periods. The subfossil shell samples used in this initial framework were *A. islandica* already established by sclerochronological cross-dating, radiocarbon dating, subfossil evidence, lithology, biostratigraphy, and AAG of other material in the same horizon (Table 1; Butler et al., 2009, 2013; Estrella-Martinez, 2019; Preece et al., 2020; Hamblin et al., 1997; Supplementary information Table S2). The iOSL was sampled, when possible, from late ontogeny for consistency of results. Samples were prepared as outlined in sections 2 and 3.5.

In a closed system the FAA and THAA D/L values are highly correlated and indicate that both fractions of amino acids degrade predictably. From the high temperature experiments (Sect. 3.3) Asx and Ser were the fastest racemisers, meaning that they should provide higher temporal resolution for dating more recent specimens. Glx, Val and Phe show slower racemisation (Supplementary information, Fig. S3), thus they may be able to separate Early Pleistocene and Late Pliocene shells and to date earlier in the Pliocene period. In our subfossil samples the FAA and THAA D/L show a high co-variance for Asx, and good correlation of THAA Glx, Ser and Asx (Fig. 12), indicating that subfossil samples follow a predictable degradation pattern.

In some amino acid parameters there seems to be different degradation patterns when comparing the high temperature experiments and subfossils (Supplementary information Fig. S7). This has been seen before in other biominerals (e.g. Tomiak et al., 2013; Dickinson et al., 2019; Baldreki et al., 2024), and may be due either to limitations of these high temperature experiments, or different degradation pathways which are enabled under high temperature conditions. Both preclude using

502 this high temperature dataset to calculate kinetic parameters for this biomineral. The 24 shells from Easton Wood (shells S)
503 show tight clustering of D/L values for 19 shells, while 4 specimens have lower D/L Asx and Val, and one specimen has higher
504 FAA Val and Ala D/L values than the cluster (Supplementary information, Fig. S8). In addition, these shells also have a
505 different percentage composition of amino acid (Asx, Glx, Phe, Ala), indicating that the closed system behaviour of these five
506 shells may have been compromised (Preece and Penkman, 2005; Penkman et al., 2007; Penkman and Wenban-Smith, 2013;
507 Demarchi et al., 2015). Therefore, we removed these five specimens from the framework (Fig. 12). Nevertheless, these tests
508 have shown that D/L values and amino acid composition are useful tools to identify outliers, providing a more accurate
509 framework for future analyses.

510 While the IcP framework is richer in the Holocene period and very limited for the Pleistocene, the Late Pliocene, Early
511 Pleistocene and Mid-Holocene samples are well-separated for the amino acids presented here, showing that it is possible to
512 distinguish between Pleistocene and Holocene samples using *A. islandica* (Fig. 12). However, using Glx and Val (Figs. 12a,
513 c, d) it is not possible to distinguish the modern and post-medieval shells. In the Asx and Ser plot (Fig. 12b) the modern, post-
514 medieval and Late Holocene (Walker et al., 2019) shells are better separated, although some overlap is still present. In this
515 plot, the THAA Ser values for the Late Pliocene and Early Pleistocene shells are undetected or lower than in modern shells,
516 because free Ser naturally decomposes with age as previously shown in the heating experiments (Sect. 3.3) and in other
517 biominerals (Penkman et al., 2008; Penkman, 2010; Crisp et al., 2013; Kaufman et al., 2013; Demarchi et al., 2013, 2015;
518 Ryan et al., 2020).

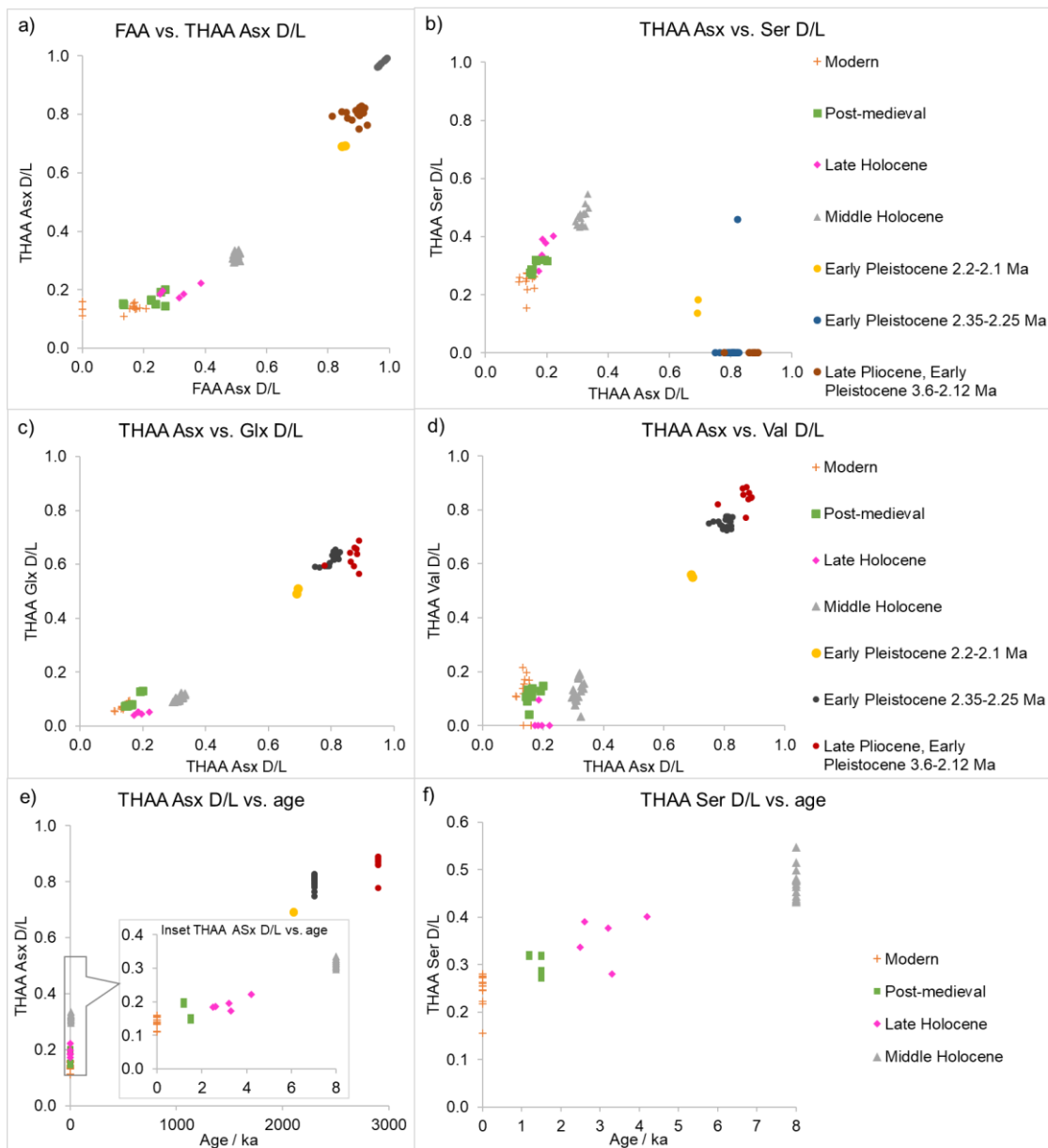


Figure 12. a) FAA vs. THAA Asx D/L; b) THAA Asx vs. Ser D/L; c) THAA Asx vs. Glx D/L; d) THAA Asx vs. Val D/L; e) THAA Asx D/L vs. age and inset focusing on the last 8 ka; f) THAA Ser D/L vs. age of modern, post-medieval, Late Holocene, Middle Holocene, Early Pleistocene and Late Pliocene *A. islandica* shells. D/L values for the slower racemising amino acids (e.g. Glx, Val) span the Quaternary period, while the faster racemising amino acids (e.g. Asx, Ser) allow temporal resolution within the Holocene.

These preliminary results indicate that it is possible to use the IcP in the iOSL of *A. islandica* for AAG of Quaternary shells. The Late Pliocene and Early Pleistocene shells have very high D/Ls for the fast racemiser Asx in (FAA Asx D/L ~0.85-0.99; THAA Asx D/L ~0.69-0.90), approaching the end-point for using Asx in AAG (Torres et al., 2013; Demarchi et al., 2013). Glx and Val D/L values were lower (FAA Glx D/L ~0.62-0.75, Val D/L ~0.75-0.95; THAA Glx D/L ~0.50-0.66, Val D/L ~0.56-0.88) meaning that there is potential to use these slower racemisers to date shells further back into the Pleistocene and Late Pliocene (Fig. 12c, d; Penkman et al., 2007; Reichert et al., 2011; Hendy et al., 2012; Torres et al., 2013; Demarchi et al., 2013; Millman et al., 2022). On the Holocene timescale, the fast racemisers Asx and Ser provide reliable D/L separation between the Middle and Late Holocene (Fig. 12f). Modern samples have a slight overlap with post-medieval shells in THAA Ser and Asx, meaning that the resolution of AAG for *A. islandica* for these amino acids may be approx. 1500-2000 years during the Middle and Late Holocene in the temperate-cold climate of the North Sea. Given the non-linear nature of AAG, the resolution will be reduced into the Pleistocene, but further analyses are required to assess the resolution. If samples date from the last ~50 ka, then radiocarbon dating will provide a higher resolution dating method compared to AAG in the temperate-cold environment where *A. islandica* typically lives, although it requires correction for the marine reservoir effect (Hajdas et al., 2021). Nevertheless, AAG using the IcP of the iOSL of *A. islandica* has the potential to discriminate Middle and Late Holocene samples, and further back into the Early Pleistocene and Late Pliocene.

3.7 AAG rangefinding of undated shells

Since the Middle and Late Holocene, important cultural transitions and palaeoenvironmental and ecological changes, both natural and human-induced, have taken place in the North Sea and Iceland and had an impact on the marine ecosystem (for example the Mesolithic-Neolithic transition, the settlements of Vikings in Iceland, and the Industrial Revolution in Northern Europe (Andersen, 2000; Ahronson, 2012; Poulsen, 2008). The palaeoenvironmental record contained within subfossil *A. islandica* provides a unique way to study these important transitions, but dating is required to identify potentially relevant shells. As part of the ERC SEACHANGE project, over twenty thousand *A. islandica* shells were collected from the North Sea and Iceland seafloors during research cruise DY150 in 2022, with the aim to use these for geochemical and sclerochronological studies (Scourse et al., 2022). Here we explore the potential for rangefinding age estimates of individual dead shells by AAG. The initial IcPD AAG framework showed the potential to provide dating of shells with resolution of 1500-2000 years during the Middle and Late Holocene. The rangefinding is expected to narrow down the age of the shells collected from the North Sea and Iceland seafloors (Supplementary information Table S2).

The AAG age rangefinding was carried out on the iOSL laid down during late ontogeny of 160 shells (Fig. 13; Supplementary information Table S2). The AAG dating determined that these shells likely span the Middle and Late Holocene, with both the Asx and Ser D/L values in agreement with this time period. In cases where there was agreement between the three most useful

parameters for the Holocene (FAA Asx D/L, THAA Asx D/L, and THAA Ser D/L), the narrowest age range possible was assigned (Fig. 13). It is noted that there are a few shells that overlap between age periods, likely due to the resolution of AAG. In case of agreement of two of the three D/L values, a wider age range was assigned. For example, shell Ic22200193 showed correlation with Late Holocene for the THAA Asx and Ser D/L, but the FAA Asx D/L value overlapped between the Late Holocene and post-medieval age; due to the agreement of two of the three parameters with the Late Holocene (which includes post-medieval), this shell was assigned an age range correlating with this stage. Shell FG22202523 showed THAA Asx D/L indicating a modern age, but FAA Asx D/L and THAA Ser D/L overlap between modern and post-medieval age, thus a post-medieval-modern age range was assigned. These three screening methods resulted in 93 shells with a narrower age range and 67 shells with a wider age range (either because of agreement of two of the three D/L, or overlap of D/L values between age ranges). There were four shells, Ic22201300, Ic2220035, Ic22200194, Ic22202048, which showed D/L values consistently higher than the Late Holocene shells but lower than the Mid-Holocene shells; thus, they were categorised as older than ~4 ka and younger than ~8 ka in age ($8 \text{ ka} < \text{shells} > 4 \text{ ka}$). Ten shells from the Fladen Ground exhibited THAA Asx and Ser D/L values slightly higher than the Mid-Holocene D/L values, thus they were categorised as Early Holocene or older. The results of AAG rangefinding of *A. islandica* shows that this technique is able to narrow down the ages of shells, assigning 10 shells to the Early Holocene or older, seven shells as younger than ~8 ka and older than ~4 ka ($8 \text{ ka} < \text{shells} > 4 \text{ ka}$), 23 shells to the Late Holocene, 34 shells to post-medieval age, and 86 modern shells. These analyses provide an initial age range for *A. islandica* shells that, depending on the time period of interest, can then enable selection of appropriate shells for more accurate radiocarbon dating and, consequently, better constrained sclerochronological crossdating.

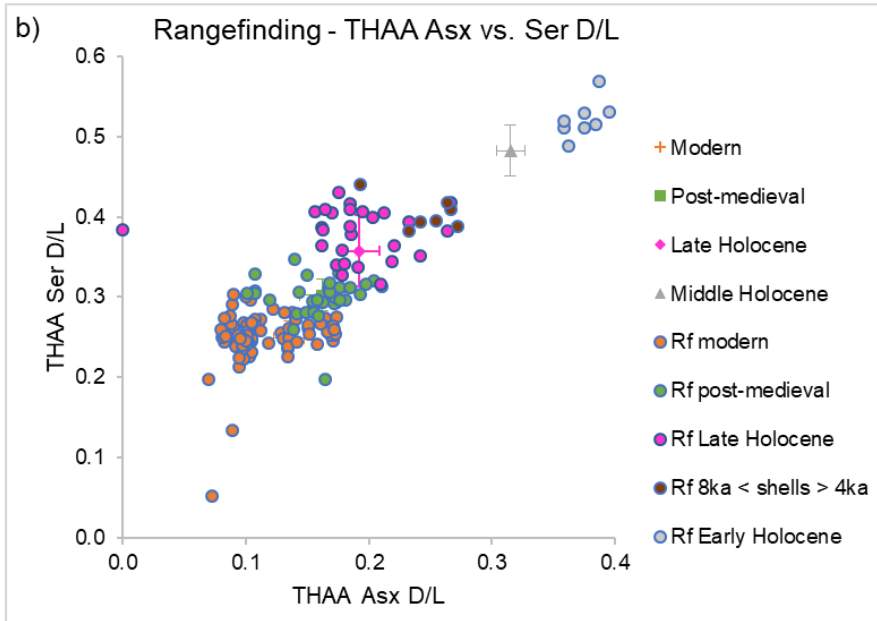
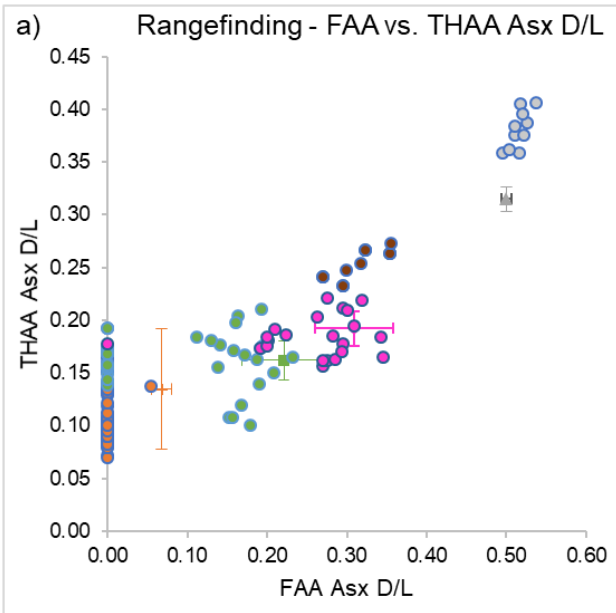


Figure 13. Rangefinding (Rf) of *A. islandica* shells within the IcPD framework (a) FAA vs. THAA Asx D/L, (b) THAA Asx vs. Ser D/L. Modern samples are in orange, post-medieval in green, Late Holocene shells in pink, shells older than ~4 ka and younger than ~8 ka (8 ka < shells > 4 ka) in brown, and Early Holocene in grey.

578 4 Conclusion

579 A protocol for the analysis of intra-crystalline chiral amino acids for amino acid geochronology (AAG) of the bivalve *A.*
580 *islandica* has been established. The three-layer microstructure of the shell has been investigated to determine which layer
581 would be most applicable to AAG. The intra-crystalline protein (IcP) fraction was successfully isolated with NaOCl oxidation
582 for 48 h. This analysis highlighted different amino acid compositions between the three layers (oOSL, iOSL and ISL), meaning
583 that for reliable dating a single microstructural layer should be sampled. Heating experiments at 140°C showed that the protein
584 fraction in the inner layer ISL is more prone to peptide bond hydrolysis than the outer layers, possible due to the high
585 composition of labile amino acids in this layer. Conversely, the outer layers show low loss and decomposition of amino acids.
586 Nevertheless, all three layers show good co-variance between FAA and THAA D/L and behave as a closed system. The iOSL
587 layer is recommended for AAG because it is already used for isotopic and sclerochronological studies. The oOSL, the
588 outermost layer, is more exposed to the external environment and marine organisms and is thinner than the iOSL, thus harder
589 to sample. Samples of early and late ontogeny in modern, post-medieval and Mid-Holocene shells did not show a consistent
590 pattern of composition and D/L, thus the resolution and sensitivity of AAG is too low for sclerochronological studies *within*
591 *A. islandica* shells of this age. The optimised method of analysis of the iOSL, following bleaching for 48 h, was applied to
592 Quaternary and Late Pliocene subfossils, providing an initial dating framework, with the fast racemisers Asx and Ser able to
593 distinguish Mid-Holocene from post-medieval/modern samples, providing a tentative resolution for AAG of *A. islandica* of
594 approx. 1500 years in the Late Holocene. The slower racemising amino acids are able to date back to at least the Late Pliocene,
595 and Val and Glx can separate Pliocene from Early Pleistocene specimens. Rangefinding of 160 undated shells showed that
596 AAG can securely separate between modern, post-medieval (~1100-1700 CE), Late Holocene (4-1 ka), Mid-Holocene (~8 ka)
597 and Early Holocene (>8 ka) shells. Further analyses are required to expand the framework and better establish the age
598 resolution for this biomineral, but these initial promising results indicate that the intra-crystalline fraction of the iOSL in *A.*
599 *islandica* is a reliable biomineral for AAG dating of marine deposits during the Quaternary and Late Pliocene periods, and
600 therefore for rangefinding collections of *A. islandica* shells of unknown age.

601 Author contribution

602 Conceptualisation: Kirsty E. H. Penkman, James D. Scourse

603 Data curation: Martina L. G. Conti

604 Formal analysis: Martina L. G. Conti, Kirsty E. H. Penkman

605 Funding acquisition: Kirsty E. H. Penkman, James D. Scourse

606 Investigation: Martina L. G. Conti, Kirsty E. H. Penkman

607 Methodology: Martina L. G. Conti, Kirsty E. H. Penkman
 608 Project administration & supervision: Kirsty E.H. Penkman, James D. Scourse
 609 Resources: Kirsty E. H. Penkman, Martina L. G. Conti, Paul G. Butler, David J. Reynolds, Tamara Trofimova, James D.
 610 Scourse
 611 Validation: Martina L. G. Conti, Paul G. Butler, David J. Reynolds, Tamara Trofimova, James D. Scourse, Kirsty E. H.
 612 Penkman
 613 Visualisation: Martina L. G. Conti, Kirsty E. H. Penkman
 614 Writing - original draft preparation: Martina L. G. Conti, Kirsty E. H. Penkman
 615 Writing - review and editing: Martina L. G. Conti, Kirsty E. H. Penkman, Paul G. Butler, David J. Reynolds, Tamara
 616 Trofimova, James D. Scourse

617 **Competing interests**

618 Kirsty E. H. Penkman is an associate editor of the journal.

619 **Acknowledgments**

620 The SEACHANGE Synergy Project has received funding from the European Research Council (ERC) under the European
 621 Union’s Horizon 2020 research and innovation programme (Grant Agreement No 856488).

622 Iceland radiocarbon dates were funded by the EU Framework 6 MILLENNIUM Integrated Project ‘European climate of the
 623 last millennium’ (SUSTDEV-2004-3.1.4.1, 017008-2).

624 North Sea radiocarbon dates were funded by the European Union Fifth Framework HOLSMEER project (EVK2-CT-2000-
 625 00060) and the United Kingdom Natural Environment Research Council standard research grant (NER/A/S/2002/00809).

626 Collection of the Easton Wood shells was funded by the European Research Council (ERC) under the European Union’s
 627 Horizon 2020 research and innovation programme (Grant Agreement No 865222). Thanks to Dr. Dustin White, Dr. R. Preece,
 628 Mr. Tim Holt-Wilson and Mr. Matthew Jeffries for collecting the shells from Easton Wood.

629 Thanks to Mr. J. Scolding, Dr. Anna Genelt-Yanovskaya, Prof. Elizabeth Harper for providing some of the samples. Thanks
 630 to Dr. Niklas Hausmann for discussing initial sampling techniques and for providing samples. Dr S. Presslee and Mr. M. von
 631 Tersch are thanked for initial laboratory training and Ms. S. Taylor for administrative support. Many thanks to Dr. Lucy
 632 Wheeler, Dr. Marc Dickinson & Ms. C. Båldreki for helpful comments on an initial version of this manuscript.

633 **Open access policy**

634 For the purpose of open access, the author has applied a Creative Commons Attribution (CC BY) licence to any Author
635 Accepted Manuscript version arising from this submission.

636 **Data availability**

637 Data in this study has been included in the Supplementary information Table S2 and all amino acid data from this study will
638 be made available through the NOAA repository upon publication: <https://www.ncei.noaa.gov/pub/data/paleo/aar/>

639 **References**

- 640 Abelson, P.H. (1955) Organic constituents of fossils. *Carnegie Institute of Washington Year Book*, 54, 107-9
- 641 Agbaje, O.B.A., Shir, I.B., Zax, D.B., Schidt, A. & Jacob, D.E. (2018) Biomacromolecules within bivalve shells: Is chitin
642 abundant? *Acta Biomaterialia*, 80, 176-187. <https://doi.org/10.1016/j.actbio.2018.09.009>
- 643 Ahronson, K. (2012) Seljaland: archaeology, palaeoecology and tephrochronology. In Larsen G, Eiríksson J (eds.) *Holocene*
644 *Tephrochronology. Applications in South Iceland*. Field Guide. *Quaternary Research Association*, London. pp 61-66.
- 645 Alves, E. Q., Macario, K., Ascough, P. & Bronk Ramsey, C. (2018). The worldwide marine radiocarbon reservoir effect:
646 Definitions, mechanisms, and prospects. *Reviews of Geophysics*, 56, 278–305. <https://doi.org/10.1002/2017RG000588>
- 647 Andersen, SH 2000. ‘Køkkenmøddinger’ (shell middens) in Denmark: A survey. proceedings of the Prehistoric Society 66,
648 361–84.
- 649 Bada, J. L. (1972). Kinetics of racemization of amino acids as a function of pH. *Journal of the American Chemical Society*,
650 94(4), 1371–1373.
- 651 Bada, J. L., Shou, M. Y., Man, E. H., & Schroeder, R. A. (1978). Decomposition of hydroxy amino acids in foraminiferal tests;
652 kinetics, mechanism and geochronological implications. *Earth and Planetary Science Letters*, 41(1), 67–76.
653 [https://doi.org/10.1016/0012-821X\(78\)90042-0](https://doi.org/10.1016/0012-821X(78)90042-0)
- 654 Baldreki, C., Burnham, A., Conti, M., Wheeler, L., Simms, M. J., Barham, L., White, T. S., & Penkman, K. (2024).
655 Investigating the potential of African land snail shells (Gastropoda: Achatininae) for amino acid geochronology. *Quaternary*
656 *Geochronology*, 79. <https://doi.org/10.1016/j.quageo.2023.101473>

657 Baleka, S., Herridge, V. L., Catalano, G., Lister, A. M., Dickinson, M. R., di Patti, C., Barlow, A., Penkman, K. E. H., Hofreiter,
658 M., & Pajmians, J. L. A. (2021). Estimating the dwarfing rate of an extinct Sicilian elephant. *Current Biology*, 31(16), 3606-
659 3612.e7. <https://doi.org/10.1016/j.cub.2021.05.037>

660 Bhattacharyya, S. K., & Banerjee, A. B. (1974). D-amino acids in the cell pool of Bacteria. *Folia Microbiol*, 19, 43–50.

661 Brand U, Morrison JO. Paleocene #6. Biogeochemistry of fossil marine invertebrates. *Geoscience Canada*. 1987
662 Jun;14(2):85-107.

663 Bridgland, D. R., Harding, P., Allen, P., Candy, I., Cherry, C., George, W., Horne, D. J., Keen, D. H., Penkman, K. E. H.,
664 Preece, R. C., Rhodes, E. J., Scaife, R., Schreve, D. C., Schwenninger, J.-L., Slipper, I., Ward, G. R., White, M. J., White, T.
665 S., & Whittaker, J. E. (2013). An enhanced record of MIS 9 environments, geochronology and geoarchaeology: data from
666 construction of the High Speed 1 (London–Channel Tunnel) rail-link and other recent investigations at Purfleet, Essex, UK.
667 *Proceedings of the Geologists' Association*, 124(3), 417–476. <https://doi.org/10.1016/j.pgeola.2012.03.006>

668 Bright, J., & Kaufman, D. S. (2011). Amino acids in lacustrine ostracodes, part III: Effects of pH and taxonomy on
669 racemization and leaching. *Quaternary Geochronology*, 6(6), 574–597. <https://doi.org/10.1016/j.quageo.2011.08.002>

670 BGS - British Geological Survey, Red Crag Formation. <https://data.bgs.ac.uk/id/Lexicon/NamedRockUnit/RCG> (accessed 16
671 Feb 2024).

672 Brooks, A. S., Hare, P. E., Kokis, J. E., Miller, G. H., Ernst, R. D., & Wendorf, F. (1990). Dating Pleistocene archeological
673 sites by protein diagenesis in ostrich eggshell. *Science*, 248(4951), 60–64. <https://www.science.org>

674 Brosset, C., Höche, N., Shirai, K., Nishida, K., Mertz-Kraus, R., & Schöne, B. R. (2022). Strong coupling between biomineral
675 morphology and Sr/Ca of *Arctica islandica* (Bivalvia)—Implications for shell Sr/Ca-based temperature estimates. *Minerals*,
676 12(5). <https://doi.org/10.3390/min12050500>

677 Butler, P. G., Richardson, C. A., Scourse, J. D., Witbaard, R., Schöne, B. R., Fraser, N. M., Wanamaker, A. D., Bryant, C. L.,
678 Harris, I., & Robertson, I. (2009). Accurate increment identification and the spatial extent of the common signal in five *Arctica*
679 *islandica* chronologies from the Fladen Ground, northern North Sea. *Paleoceanography*, 24(2).
680 <https://doi.org/10.1029/2008PA001715>

681 Butler, P. G., Wanamaker, A. D., Scourse, J. D., Richardson, C. A., & Reynolds, D. J. (2013). Variability of marine climate
682 on the North Icelandic Shelf in a 1357-year proxy archive based on growth increments in the bivalve *Arctica islandica*.
683 *Palaeogeography, Palaeoclimatology, Palaeoecology*, 373, 141–151. <https://doi.org/10.1016/j.palaeo.2012.01.016>

684 Checa, A. (2000) A new model for periostracum and shell formation in Unionidae (Bivalvia, Mollusca). *Tissue & Cell*, 32(5),
685 405-406. doi: 10.1054/tice.2000.0129

686 Crippa, G., Azzarone, M., Bottini, C., Crespi, S., Felletti, F., Marini, M., Petrizzo, M. R., Scarponi, D., Raffi, S., & Raineri,
687 G. (2019). Bio-and lithostratigraphy of lower Pleistocene marine successions in western Emilia (Italy) and their implications
688 for the first occurrence of *Arctica islandica* in the Mediterranean Sea. *Quaternary Research (United States)*, 92(2), 549–569.
689 <https://doi.org/10.1017/qua.2019.20>

690 Crisp, M. K. (2013). Amino acid racemization dating: Method development using African ostrich (*Struthio camelus*) eggshell.
691 PhD thesis, University of York.

692 Crisp, M., Demarchi, B., Collins, M., Morgan-Williams, M., Pilgrim, E., & Penkman, K. (2013). Isolation of the intra-
693 crystalline proteins and kinetic studies in *Struthio camelus* (ostrich) eggshell for amino acid geochronology. *Quaternary*
694 *Geochronology*, 16, 110–128. <https://doi.org/10.1016/j.quageo.2012.09.002>

695 Davies, B. J., Bridgland, D. R., Roberts, D. H., Cofaigh, C. Ó., Pawley, S. M., Candy, I., Demarchi, B. (2009). The age and
696 stratigraphic context of the Easington Raised Beach, County Durham, UK. *Proceedings of the Geologists' Association*, 120,
697 4, 183-198.

698 Demarchi, B., Clements, E., Coltorti, M., van de Locht, R., Kröger, R., Penkman, K., & Rose, J. (2015). Testing the effect of
699 bleaching on the bivalve *Glycymeris*: A case study of amino acid geochronology on key Mediterranean raised beach deposits.
700 *Quaternary Geochronology*, 25, 49–65. <https://doi.org/10.1016/j.quageo.2014.09.003>

701 Demarchi, B., Collins, M. J., Tomiak, P. J., Davies, B. J., & Penkman, K. E. H. (2013b). Intra-crystalline protein diagenesis
702 (IcPD) in *Patella vulgata*. Part II: Breakdown and temperature sensitivity. *Quaternary Geochronology*, 16, 158–172.
703 <https://doi.org/10.1016/j.quageo.2012.08.001>

704 Demarchi, B. Geochronology of coastal prehistoric environments: a new closed system approach using amino acid
705 racemisation. PhD thesis, University of York.

706 Demarchi, B., Rogers, K., Fa, D. A., Finlayson, C. J., Milner, N., & Penkman, K. E. H. (2013a). Intra-crystalline protein
707 diagenesis (IcPD) in *Patella vulgata*. Part I: Isolation and testing of the closed system. *Quaternary Geochronology*, 16, 144–
708 157. <https://doi.org/10.1016/j.quageo.2012.03.016>

709 Dickinson, M. R., Lister, A. M., & Penkman, K. E. H. (2019). A new method for enamel amino acid racemization dating: A
710 closed system approach. *Quaternary Geochronology*, 50, 29–46. <https://doi.org/10.1016/j.quageo.2018.11.005>

711 Dominguez, J. G., Kosnik, M. A., Allen, A. P., Hua, Q., Jacob, D. E., Kaufman, D. S., & Whitacre, K. (2016). Time-averaging
712 and stratigraphic resolution in death assemblages and Holocene deposits. *Source: PALAIOS*, 31(11), 564–575.
713 <https://doi.org/10.2307/26780062>

714 Dunca, E., Mutvei, H., Göransson, P., Mörrh, C. M., Schöne, B. R., Whitehouse, M. J., Elfman, M., & Baden, S. P. (2009).
715 Using ocean quahog (*Arctica islandica*) shells to reconstruct palaeoenvironment in Öresund, Kattegat and Skagerrak, Sweden.
716 *International Journal of Earth Sciences*, 98(1), 3–17. <https://doi.org/10.1007/s00531-008-0348-6>

717 Estrella-Martínez, J., Ascough, P. L., Schöne, B. R., Scourse, J. D., & Butler, P. G. (2019). 8.2 ka event North Sea hydrography
718 determined by bivalve shell stable isotope geochemistry. *Scientific Reports*, 9(1), 1–9. [https://doi.org/10.1038/s41598-019-](https://doi.org/10.1038/s41598-019-43219-1)
719 43219-1

720 Estrella-Martínez, J. (2019). Holocene climate variability in UK waters based on *Arctica islandica* sclerochronology. PhD
721 thesis, Bangor University.

722 Eyles, N., McCabe, A. M., & Bowen, D. Q. (1994). The stratigraphic and sedimentological significance of Late Devensian ice
723 sheet surging in Holderness, Yorkshire, U.K. *Quaternary Science Reviews*, 13(8), 727–759. [https://doi.org/10.1016/0277-](https://doi.org/10.1016/0277-3791(94)90102-3)
724 3791(94)90102-3

725 Goodfriend, G. A., Hare, P. E., & Druffel, E. R. M. (1992). Aspartic acid racemization and protein diagenesis in corals over
726 the last 350 years. In *Geochimica et Cosmochimica Acta* (Vol. 56, pp. 3847–3850). [https://doi.org/10.1016/0016-](https://doi.org/10.1016/0016-7037(94)00324-F)
727 7037(94)00324-F

728 Goodfriend, G. A., & Weidman, C. R. (2001). Ontogenetic trends in aspartic acid racemization and amino acid composition
729 within modern and fossil shells of the bivalve *Arctica*. *Geochimica et Cosmochimica Acta*, 65(12), 1921–1932.
730 [https://doi.org/10.1016/S0016-7037\(01\)00564-6](https://doi.org/10.1016/S0016-7037(01)00564-6)

731 Goodfriend, G. A., Flessa, K. W., & Hare, P. E. (1997). Variation in amino acid epimerization rates and amino acid
732 composition among shell layers in the bivalve *Chione* from the Gulf of California. *Geochimica et Cosmochimica Acta*, 61, 7,
733 1487–1493.

734 Goodfriend, G. A., Kashgarian, M., & Harasewych, M. G. (1995). Use of aspartic acid racemization and post-bomb ¹⁴C to
735 reconstruct growth rate and longevity of the deep-water slit shell *Entemnotrochus adansonianus*. *Geochimica et Cosmochimica*
736 *Acta*, 59(6), 1125–1129. <https://www.sciencedirect.com/science/article/pii/001670379500029Y>

737 Gries, K., Kröger, R., Kübel, C., Fritz, M., & Rosenauer, A. (2009). Investigations of voids in the aragonite platelets of nacre.
738 *Acta Biomaterialia*, 5(8), 3038–3044. <https://doi.org/10.1016/j.actbio.2009.04.017>

739 Hajdas, I., Ascough, P., Garnett, M. H., Fallon, S. J., Pearson, C. L., Quarta, G., Spalding, K. L., Yamaguchi, H., & Yoneda,
740 M. (2021). Radiocarbon dating. *Nature Reviews Methods Primers*, 1(1), 62. <https://doi.org/10.1038/s43586-021-00058-7>

741 Hamblin, R. J. O., Moorlock, B. S. P., Booth, S. J., Jeffery, & D. H., Morigi, A. N. (1997). The Red Crag and Norwich Crag
742 formations in eastern Suffolk. *Proceedings of the Geologists' Association*, 108, 11-23. [https://doi.org/10.1016/S0016-](https://doi.org/10.1016/S0016-7878(97)80002-8)
743 [7878\(97\)80002-8](https://doi.org/10.1016/S0016-7878(97)80002-8)

744 Hare, P. E. & Abelson, P. H. 1968. Racemization of amino acids in fossil shells. *Carnegie Institute of Washington Yearbook*
745 66:526-8

746 Hare PE, Mitterer RM. (1969). Laboratory simulation of amino acid diagenesis in fossils. *Carnegie Institute of Washington*
747 *Yearbook* 67:205-8

748 Haugen, J. E., & Sejrup, H. P. (1992). Isoleucine epimerization kinetics in the shell of *Arctica islandica*. *Norsk Geologisk*
749 *Tidsskrift*, 72(2), 171–180. https://foreninger.uio.no/ngf/ngt/pdfs/NGT_72_2_171-180.pdf

750 Haugen, J.-E., & Sejrup, H. P. (1990). Amino acid composition of aragonitic concholin in the shell of *Arctica islandica*.
751 *Lethaia*, 23(2), 133–141. <https://doi.org/10.1111/j.1502-3931.1990.tb01354.x>

752 Heaton, T. J., P. Köhler, M. Butzin, E. Bard, R. W. Reimer, W. E. N. Austin, C. Bronk Ramsey, P. M. Grootes, K. A. Hughen,
753 B. Kromer, P. J. Reimer, J. Adkins, A. Burke, M. S. Cook, J. Olsen, and L. C. Skinner. 2020: Marine20—The Marine
754 Radiocarbon Age Calibration Curve (0–55,000 cal BP). *Radiocarbon* 62:779–820. doi:10.1017/RDC.2020.68

755 Hendy, E. J., Tomiak, P. J., Collins, M. J., Hellstrom, J., Tudhope, A. W., Lough, J. M., & Penkman, K. E. H. (2012). Assessing
756 amino acid racemization variability in coral intra-crystalline protein for geochronological applications. *Geochimica et*
757 *Cosmochimica Acta*, 86, 338–353. <https://doi.org/10.1016/j.gca.2012.02.020>

758 IUGS International Chronostratigraphic Chart, v 2023/09 (2023) <https://stratigraphy.org/chart> (accessed 24 Feb 2024).

759 Kaufman, D. S., & Manley, W. F. (1998). A new procedure for determining DL amino acid ratios in fossils using reverse phase
760 liquid chromatography. *Quaternary Science Reviews*, 17(11), 987–1000. [https://doi.org/10.1016/S0277-3791\(97\)00086-3](https://doi.org/10.1016/S0277-3791(97)00086-3)

761 Kosnik, M. A., & Kaufman, D. S. (2008). Identifying outliers and assessing the accuracy of amino acid racemization
762 measurements for geochronology: II. Data screening. *Quaternary Geochronology*, 3(4), 328–341.
763 <https://doi.org/10.1016/j.quageo.2008.04.001>

764 Kaufman, D. S., Cooper, K., Behl, R., Billups, K., Bright, J., Gardner, K., Hearty, P., Jakobsson, M., Mendes, I., O’Leary, M.,
765 Polyak, L., Rasmussen T., Rosa, F., & Schmidt, M. (2013). Amino acid racemization in mono-specific foraminifera from
766 Quaternary deep-sea sediments. *Quaternary Geochronology*, 16, 50–61. <https://doi.org/10.1016/j.quageo.2012.07.006>.

767 Kriausakul, N., & Mitterer, R. M. (1978). Isoleucine epimerization in peptides and proteins: kinetic factors and application to
768 fossil proteins. *Science (New York, N.Y.)*, 201(4360), 1011–1014. <https://doi.org/10.1126/science.201.4360.1011>

769 Malatesta, A., & Zarlenga, F. (1986). Northern guests in the Pleistocene Mediterranean Sea. *Geologica Romana*, 25, 91–154.

770 Marchitto, T. M., Jones, G. A., Goodfriend, G. A., & Weidman, C. R. (2000). Precise temporal correlation of Holocene mollusk
771 shells using sclerochronology. *Quaternary Research*, 53(2), 236–246. <https://doi.org/10.1006/qres.1999.2107>

772 Milano, S., Nehrke, G., Wanamaker, A. D., Ballesta-Artero, I., Brey, T., & Schöne, B. R. (2017b). The effects of environment
773 on *Arctica islandica* shell formation and architecture. *Biogeosciences*, 14(6), 1577–1591. [https://doi.org/10.5194/bg-14-1577-](https://doi.org/10.5194/bg-14-1577-2017)
774 2017

775 Milano, S., Schöne, B. R., & Witbaard, R. (2017a). Changes of shell microstructural characteristics of *Cerastoderma edule*
776 (Bivalvia) — A novel proxy for water temperature. *Palaeogeography, Palaeoclimatology, Palaeoecology*, 465, 395–406.
777 <https://doi.org/10.1016/j.palaeo.2015.09.051>

778 Mitterer, R. M. (1975). Ages and diagenetic temperatures of pleistocene deposits of Florida based on isoleucine epimerization
779 in *Mercenaria*. *Earth and Planetary Science Letters*, 28(2), 275–282. [https://doi.org/10.1016/0012-821X\(75\)90237-X](https://doi.org/10.1016/0012-821X(75)90237-X)

780 Orem, C. A., & Kaufman, D. S. (2011). Effects of basic pH on amino acid racemization and leaching in freshwater mollusk
781 shell. *Quaternary Geochronology*, 6(2), 233–245. <https://doi.org/10.1016/j.quageo.2010.11.005>

782 Ortiz, J. E., Gutiérrez-Zugasti, I., Torres, T., González-Morales, M., & Sánchez-Palencia, Y. (2015). Protein diagenesis in
783 *Patella* shells: Implications for amino acid racemisation dating. *Quaternary Geochronology*, 27, 105–118.
784 <https://doi.org/10.1016/j.quageo.2015.02.008>

785 Ortiz, J. E., Sánchez-Palencia, Y., Gutiérrez-Zugasti, I., Torres, T., & González-Morales, M. (2018). Protein diagenesis in
 786 archaeological gastropod shells and the suitability of this material for amino acid racemisation dating: *Phorcus lineatus* (da
 787 Costa, 1778). *Quaternary Geochronology*, 46, 16–27. <https://doi.org/10.1016/j.quageo.2018.02.002>

788 Ortiz, J. E., Torres, T., & Pérez-González, A. (2013). Amino acid racemization in four species of ostracodes: Taxonomic,
 789 environmental, and microstructural controls. *Quaternary Geochronology*, 16, 129–143.
 790 <https://doi.org/10.1016/j.quageo.2012.11.004>

791 Ortiz, J. E., Torres, T., González-Morales, M. R., Abad, J., Arribas, I., Fortea, F. J., Garcia-Belenguer, F., & Gutiérrez-Zugasti,
 792 I. (2009). The aminochronology of man-induced shell middens in caves in Northern Spain. *Archaeometry*, 51(1), 123–139.
 793 <https://doi.org/10.1111/j.1475-4754.2008.00383.x>

794 Penkman, K. (2010). Amino acid geochronology: Its impact on our understanding of the Quaternary stratigraphy of the British
 795 Isles. *Journal of Quaternary Science*, 25(4), 501–514. <https://doi.org/10.1002/jqs.1346>

796 Penkman, K. E. H., Preece, R. C., Keen, D. H., Maddy, D., Schreve, D. C., & Collins, M. J. (2007). Testing the
 797 aminostratigraphy of fluvial archives: the evidence from intra-crystalline proteins within freshwater shells. *Quaternary Science*
 798 *Reviews*, 26(22–24), 2958–2969. <https://doi.org/10.1016/j.quascirev.2007.06.034>

799 Penkman, K. E. H., Kaufman, D. S., Maddy, D., & Collins, M. J. (2008). Closed-system behaviour of the intra-crystalline
 800 fraction of amino acids in mollusc shells. *Quaternary Geochronology*, 3(1–2), 2–25.
 801 <https://doi.org/10.1016/j.quageo.2007.07.001>

802 Penkman, K. E. H., & Wenban-Smith, F. (2013). Amino acid dating. In F. Wenban-Smith (Ed.), *The Ebbsfleet elephant: Excavations at Southfleet Road, Swanscombe in advance of High Speed 1, 2003–4* (Vol. 20, pp. 307–318). Oxford
 803 Archaeology.
 804

805 Poulsen, B. (2008). *Dutch Herring - An Environmental History, c. 1600–1860*. Amsterdam University.

806 Preece, R. C., & Penkman, K. E. H. (2005). New faunal analyses and amino acid dating of the Lower Palaeolithic site at East
 807 Farm, Barnham, Suffolk. *Proceedings of the Geologists' Association*, 116(3–4), 363–377. [https://doi.org/10.1016/S0016-](https://doi.org/10.1016/S0016-7878(05)80053-7)
 808 [7878\(05\)80053-7](https://doi.org/10.1016/S0016-7878(05)80053-7)

809 Preece, R. C., Meijer, T., Penkman, K. E. H., Demarchi, B., Mayhew, D. F., & Parfitt, S. A. (2020). The palaeontology and
 810 dating of the ‘Weybourne Crag’, an important marker horizon in the Early Pleistocene of the southern North Sea basin.
 811 *Quaternary Science Reviews*, 236. <https://doi.org/10.1016/j.quascirev.2020.106177>

Reynolds, D. J., Scourse, J. D., Halloran, P. R., Nederbragt, A. J., Wanamaker, A. D., Butler, P. G., Richardson, C. A., Heinemeier, J., Eiríksson, J., Knudsen, K. L., & Hall, I. R. (2016). Annually resolved North Atlantic marine climate over the last millennium. *Nature Communications*, 7(2), 201–217. <https://doi.org/10.1038/ncomms13502>

Ryan, D. D., Lachlan T. J., Murray-Wallace, C. V., & Price, D. M. (2020). The utility of single foraminifera amino acid racemization analysis for the relative dating of Quaternary beach barriers and identification of reworked sediment. *Quaternary Geochronology*, 60, 101103. <https://doi.org/10.1016/j.quageo.2020.101103>.

Schöne, B. R., Freyre Castro, A. D., Fiebig, J., Houk, S. D., Oschmann, W., & Kröncke, I. (2004). Sea surface water temperatures over the period 1884–1983 reconstructed from oxygen isotope ratios of a bivalve mollusk shell (*Arctica islandica*, southern North Sea). *Palaeogeography, Palaeoclimatology, Palaeoecology*, 212(3–4), 215–232. <https://doi.org/10.1016/j.palaeo.2004.05.024>

Schöne, B. R., & Fiebig, J. (2009). Seasonality in the North Sea during the Allerød and Late Medieval Climate Optimum using bivalve sclerochronology. *International Journal of Earth Sciences*, 98(1), 83–98. <https://doi.org/10.1007/s00531-008-0363-7>

Schöne, B. R. (2013). *Arctica islandica* (Bivalvia): A unique paleoenvironmental archive of the northern North Atlantic Ocean. *Global and Planetary Change*, 111, 199–225. <https://doi.org/10.1016/j.gloplacha.2013.09.013>

Schöne, B. R., & Huang, Q. (2021). Ontogenetic $\delta^{15}\text{N}$ Trends and Multidecadal Variability in Shells of the Bivalve Mollusk, *Arctica islandica*. *Frontiers in Marine Science*, 8(748593), 1–15. <https://doi.org/10.3389/fmars.2021.748593>

Schöne, B. R., Dunca, E., Fiebig, J., & Pfeiffer, M. (2005b). Mutvei’s solution: An ideal agent for resolving microgrowth structures of biogenic carbonates. *Palaeogeography, Palaeoclimatology, Palaeoecology*, 228(1–2), 149–166. <https://doi.org/10.1016/j.palaeo.2005.03.054>

Schöne, B. R., Fiebig, J., Pfeiffer, M., Gleß, R., Hickson, J., Johnson, A. L. A., Dreyer, W., & Oschmann, W. (2005a). Climate records from a bivalved Methuselah (*Arctica islandica*, Mollusca; Iceland). *Palaeogeography, Palaeoclimatology, Palaeoecology*, 228(1–2), 130–148. <https://doi.org/10.1016/j.palaeo.2005.03.049>

Scourse, J. D., Wanamaker, A. D., Weidman, C., Heinemeier, J., Reimer, P. J., Butler, P. G., Witbaard, R., & Richardson, C. A. (2012): The marine radiocarbon bomb pulse across the temperate North Atlantic: A compilation of $\delta^{14}\text{C}$ time histories from *Arctica islandica* growth increments. *Radiocarbon* 54:165–186. doi:10.2458/azu_js_rc.v54i2.16026

Scourse, J. D., Afrifa, K., Byrne, L., Crowley, D., Earland, J. L., Ehmen, T., Frøslev, T. G., Greenall, C., Harland, J., Heard, Z., Höche, N., Holman, L. E., Huang, Q., Langkjær, E. M. R., Mason, M., Nelson, E., Nemeth, Z., Reynolds, D., Robson, H.

839 K., Roman-Gonzalez, A., Scherer, P., Scolding, J., Short, J., Wilkin, J. T. R., Wilson, D. R. (2022). DY150 Cruise report.
840 <https://seachange-erc.eu/research/north-west-european-research-cruise>

841 Sejrup, H. P., & Haugen, J. -E. (1994). Amino acid diagenesis in the marine bivalve *Arctica islandica* Linné from northwest
842 European sites: Only time and temperature? *Journal of Quaternary Science*, 9(4), 301–309.
843 <https://doi.org/10.1002/jqs.3390090402>

844 Stuiver, M., & Reimer, P.J. (1993): Extended ^{14}C data base and revised CALIB 3.0 ^{14}C age calibration program. *Radiocarbon*,
845 35, 215–230. doi:10.1017/S0033822200013904

846 Sykes, G. A., Collins, M. J., & Walton, D. I. (1995). The significance of a geochemically isolated intracrystalline organic
847 fraction within biominerals. *Organic Geochemistry*, 23(11–12), 1059–1065. [https://doi.org/10.1016/0146-6380\(95\)00086-0](https://doi.org/10.1016/0146-6380(95)00086-0)

848 Tomiak, P. J., Andersen, M. B., Hendy, E. J., Potter, E. K., Johnson, K. G., & Penkman, K. E. H. (2016). The role of skeletal
849 micro-architecture in diagenesis and dating of *Acropora palmata*. *Geochimica et Cosmochimica Acta*, 183, 153–175.
850 <https://doi.org/10.1016/j.gca.2016.03.030>

851 Tomiak, P. J., Penkman, K. E. H., Hendy, E. J., Demarchi, B., Murrells, S., Davis, S. A., McCullagh, P., & Collins, M. J.
852 (2013). Testing the limitations of artificial protein degradation kinetics using known-age massive *Porites* coral skeletons.
853 *Quaternary Geochronology*, 16, 87–109. <https://doi.org/10.1016/j.quageo.2012.07.001>

854 Torres, T., Ortiz, J. E., & Arribas, I. (2013). Variations in racemization/epimerization ratios and amino acid content of
855 *Glycymeris* shells in raised marine deposits in the Mediterranean. *Quaternary Geochronology*, 16, 35–49.
856 <https://doi.org/10.1016/j.quageo.2012.11.002>

857 Towe, K. M., & Thompson, G. R. (1972). The structure of some bivalve shell carbonates prepared by ion-beam thinning - A
858 comparison study. *Calcified Tissue Research*, 10, 38–48.

859 Trofimova, T., Milano, S., Andersson, C., Bonitz, F. G. W., & Schöne, B. R. (2018). Oxygen isotope composition of *Arctica*
860 *islandica* aragonite in the context of shell architectural organization: Implications for paleoclimate reconstructions.
861 *Geochemistry, Geophysics, Geosystems*, 19(2), 453–470. <https://doi.org/10.1002/2017GC007239>

862 Vallentyne, J. R. 1964. Biogeochemistry of organic matter II: Thermal reaction kinetics and transformation products of amino
863 compounds. *Geochimica et Cosmochimica Acta* 28:157-88

864 Walker, M., Head, M. J., Lowe, J., Berkelhammer, M., Björck, S., Cheng, H., Cwynar, L. C., Fisher, D., Gkinis, V., Long, A.,
865 Newnham, R., Rasmussen, S. O., & Weiss, H. (2019). Subdividing the Holocene Series/Epoch: formalization of stages/ages
866 and subseries/subepochs, and designation of GSSPs and auxiliary stratotypes. *Journal of Quaternary Science*, 34(3), 173–186.
867 <https://doi.org/10.1002/jqs.3097>

868 Walton D. 1998. Degradation of intracrystalline proteins and amino acids in fossil brachiopods. *Organic Geochemistry* 28:389-
869 410

870 Wanamaker Jr., A. D., Butler, P. G., Scourse, J. D., Heinemeier, J., Eiríksson, J., Knudsen, K. L., & Richardson, C. A. (2012).
871 Surface changes in the North Atlantic meridional overturning circulation during the last millennium. *Nature Communications*,
872 3(899), 1–7. <https://doi.org/10.1038/ncomms1901>

873 Wheeler, L. J., Penkman, K. E. H., & Sejrup, H. P. (2021). Assessing the intra-crystalline approach to amino acid
874 geochronology of *Neogloboquadrina pachyderma* (sinistral). *Quaternary Geochronology*, 61(June 2020), 101131.
875 <https://doi.org/10.1016/j.quageo.2020.101131>

876 Witbaard, R., Duineveld, G. C. A., & de Wilde, P. A. W. J. (1997). A long-term growth record derived from *Arctica islandica*
877 (Mollusca, Bivalvia) from the Fladen ground (northern North Sea). *Journal of the Marine Biological Association of the United*
878 *Kingdom*, 77(3), 801–816. <https://doi.org/10.1017/s0025315400036201>